Rheological and Filtration Property Evaluations of the Nano-Based Muds for Drilling Applications in Low Temperature Environments

Rizky Novara, Roozbeh Rafati*, Amin Sharifi Haddad

School of Engineering, University of Aberdeen, Aberdeen, United Kingdom

ABSTRACT

As the search of hydrocarbon has moved to the more remote and unconventional areas, including low temperature offshore and Arctic circle, new challenges have also emerged to the life of the industry. The biggest drilling fluid-related challenge in low temperature environments, is maintaining fluid properties under an extreme temperature difference between the bottom hole and the surface. The rapid change of temperature conditions can affect mud rheological properties and reduce drilling performance. The heat released from the mud circulation system can also cause thawing of the permafrost and gas hydrate-bearing formations impacting the wellbore integrity and releasing greenhouse gases to the environment. Creating a more thermally independent drilling mud becomes one of the solutions to reduce the potential problem that may arise. The aim of this study is to address the issue by designing nano-based drilling muds that will demonstrate more thermally stable characteristics. Silica (SiO_2) and alumina (Al_2O_3) nanoparticles were used in the freshwater- and saltwater-based mud formulations at various concentrations. The mud rheological properties evaluation was conducted using a direct-reading viscometer at a temperature range from 0 to 80°C, whilst mud filtration properties was evaluated using a low-pressure filter press under 700 kPa (100 psi) differential pressure. The concentration of 0.1 wt% of each type of nanoparticles showed the optimum profile in which rheological properties were most stable across the broad temperature conditions in both the freshwater- and saltwater-based systems. The sample containing 0.1 wt% of silica also gave the lowest filtration properties in which a reduction of 8.2% was observed in the filtration loss volume.

Keywords: drilling muds; filtration; rheology; surface charges; thermal stability

INTRODUCTION

One of the biggest mud-related issues in drilling in the low temperature environments such as offshore deep-water and the Arctic circle, is maintaining the desired mud properties affected by the extreme difference between the bottom hole and surface temperatures (Hilfiger et al., 2016). In the Arctic region, the occurrence of permafrost and gas hydrate-bearing formations could cause difficulty in maintaining borehole stability. Since any drilling activity produces heat including the heat brought from the high-temperature rock formations, as a consequence, it warms up the surrounding sediments at the shallower depth up to a point at which the temperature exceeds the hydrate phase boundary causing hydrate to dissociate releasing hazardous methane gas, if not carefully treated, into the mud circulation or surrounding environment. Controlling mud temperature by reducing mud weight or through the use of more thermally stable mud becomes important when drilling through these formations (Yakushev and Collett, 1992).

Such an extreme temperature condition encountered in the Arctic drillings is also experienced in the offshore deep-water operations. Although not as low as it is in the Arctic, seabed temperatures can reach up to a minimum of -1°C (Davison et al., 1999). These conditions will affect the physical characteristics of the thermally dependent muds when flowing back from the high bottomhole temperature conditions. The conventional drilling muds normally exhibit a higher surface viscosity due to the low-temperature or sub-zero condition even before entering formations. As the drilling continues, the temperature increases and the thermal thinning behaviour will cause viscosity reduction up to the point in which the mud loses the ability to carry cutting and weighting agents, affecting the hole cleaning ability of the mud. A viscosifier will then be added to improve the overall fluid rheology. However, the mud will become excessively viscous as it returns to the low-temperature surface resulting in high equivalent circulating density (ECD) (Hilfiger et al., 2016). A high ECD is always avoided in drilling operations as it increases the pump pressure that can cause formation breakdown if the pressure of the fluid column exceeds the fracture gradient of the rock formations. To overcome this challenge, the then so-called a temperature-independent or constant-rheology mud was designed. The idea was to design a drilling mud that exhibits more thermally stable characteristics across a broad temperature conditions. This mud was initially designed for the offshore deep-water drilling applications (Davison et al., 1999; Friedheim et al., 2011; Knox et al., 2015; Lee et al., 2012; Rojas et al., 2007; van Oort et al., 2004; Young et al., 2012). Amongst the first to formulate this type of muds were Elward-Berry and Thomas, 1994, where they formulated the mud sample by mixing saltwater and polyglycerol as the continuous phase and added with some polymeric additives including starch, polyanionic cellulose, and bio-gum. The experimental results indicated an improved independence on the rheological profiles over a temperature range between 4 and 50°C. The improvement was attributed to the extensive use of polymers which were manufactured to have excellent temperature stability (Caenn et al., 2017a). Rojas et al., 2007, conducted experiments on the oil-based muds at temperatures between 0 and 100°C. They formulated three different types of mud formulations using mineral oil, synthetic, and ester as the continuous phase of the mud suspension. The results suggested that mineral oil-based mud exhibited the most stable rheological profiles compared to the other two oil-based mud formulations. Drilling muds with similar quality was also observed from the experiments conducted by Lee et al., 2012, in which they formulated mud samples in oil-based system using three different oils: paraffin, olefin, and mineral oils. As was experienced by Rojas et al., the results also demonstrated a better performance from the oil-based formulation, as indicated by a more constant plastic viscosity profile at temperatures ranging between 4 and 122°C and pressure up to 86 MPa. They concluded that the mineral oil-based mud exhibited a more constant rheological profiles across the increasing temperature and pressure compared to the other two oils. The improved thermal stability was attributed to the low thermal conductivity of the mineral oil at around 0.133 W/m.K (Nadolny and Dombek, 2017) as compared to about 0.152 W/m.K (Oyekunle and Susu, 2005) and 0.154 W/m.K (Larsson and Andersson, 2000) for paraffin and olefin, respectively.

The drawback from this thermally stable mud is that it is mostly formulated in the oil and synthetic-based mud systems due to their high lubricity and formation damage prevention benefits. However, oil itself is considered toxic and hazardous to the environment (Nesbitt and

Sanders, 1981) which may result in a higher waste management cost for mud disposal, especially when used in the Arctic region (Maunder et al., 1990; Rakhmangulov et al., 2016). For this reason, designing a drilling mud that provides similar quality in the aqueous-based system is essential to reduce the excessive use of toxic or hazardous additives in drilling muds not only for the Arctic operations but also for the offshore deepwater drillings in general.

In the last decades, an extensive amount of research has been published across various industries to determine the extent of the effect of nanoparticles on the physical, electrical, and thermal properties of working fluids, including in drilling muds (Bashir et al, 2019; Bayat[a] et al, 2014; Hendraningrat et al., 2013; Mahian et al., 2019; William et al., 2014; Rafati et al, 2018; Smith et al, 2018). Nanoparticles are added to drilling muds to alter physical characteristics and improve their flow behaviour that leads to increased efficiency of drilling operations (Dejtaradon et al, 2019, Ahmed et al, 2021). As clay minerals are mostly used in the compositions of drilling mud colloidal systems, there are two governing phenomena by which the presence of nanoparticles may affect mud properties significantly than those of bulk additive materials. The first phenomenon is the Brownian motion, which is the erratic movement of particles caused by the constant bombardment of water molecules. Solid components with smaller diameter have a greater number of particles and higher surface areas contained for a given concentration than solid components with larger diameter. This causes a reduction in the distance between them increasing the change of collision attributed to the stronger Brownian motion of particles. Hence, producing a stronger attractive force that will enhance flocculation between particles which therefore altering mud physical properties (Bayat[c], et al., 2018, Timofeeva et al., 2010; Yapici et al., 2018). The second phenomenon is the electrostatic charge imbalance on the surface layer of the clay particles. Clay mineral such as, montmorillonite in bentonite exhibits a permanently negative charge on its basal surface layers when dispersed in water (neutral pH). At the same time, nanoparticles also exhibit surface charges whose magnitudes are determined by the point zero charges (PZC) of the materials and the pH of the base fluid in which the particles are dispersed (Adair et al., 2001). As a result, the strength of the interparticle attraction force is changed, which affects the degree of flocculation and dispersion of the colloidal system, which therefore altering the physical characteristics of drilling muds.

Abdo et al. were amongst the researchers conducting extensive studies using nanoparticles in different variety of types, sizes, shapes, and concentrations in both aqueous and oil-based mud systems (Abdo, 2014; Abdo et al., 2016, 2014; Abdo and Haneef, 2013, 2012). In one of their studies, they successfully formulated a drilling mud that exhibited a more stable rheological profile at HPHT conditions. They conducted experiments evaluating mud samples containing nanoparticles across a temperature range between 43 and 188°C and pressure of up to 128 MPa. The mud samples contained a composite of zinc oxide and montmorillonite clay nanoparticles with particle size diameters from 5 to 35 nm and 20 to 50 nm, respectively. The experimental results indicated a nanocomposite concentration of 2.3 wt% observed the most significant improvement on the thermal stability indicated from the increases of up to 140% and 150% in the plastic viscosity and yield point, respectively, at temperature and pressure of 188°C and 128 MPa (Abdo et al., 2014). Mahmoud et al., 2016, conducted a rheological properties evaluation to water-based muds containing iron oxide and silica nanoparticles, with average

particle diameters of 50 and 12 nm, respectively. A concentration of 0.5 wt% of each nanoparticle was added into a base mud containing 7 wt% of bentonite. The experiments were conducted at temperatures between 49 and 93°C. The experimental results demonstrated improvements of up to 34% and 104% in the plastic viscosity from the addition of iron oxide and silica nanoparticles, respectively at temperature of 93°C. One of the more recent studies was conducted by Bayat[b] et al., 2019, who tested three types of nanoparticles, i.e., zinc oxide, titanium oxide, and silica nanoparticles, with average particle diameters of 17, 7, and 13 nm, respectively. The nanoparticles were added at concentrations between 0.01 and 0.5 wt% into a water-based mud containing 6 and 0.4 wt% of bentonite and sodium carbonate, respectively. The tests were conducted at temperatures of 25 and 50°C. The results indicated significant improvements of up to 50, 35, and 44% in plastic viscosity at 50°C from the mud samples containing zinc oxide, titanium oxide, and silica nanoparticles, respectively.

The addition of nanoparticles to drilling mud formulations has also been found to be beneficial in maintaining borehole stability by building sufficient mud cakes and reducing filtration losses. Sadeghalvaad et al., 2015, conducted a study evaluating the filtration properties of nano-based drilling muds. In their experiments, they used a composite of polyacrylamide and titanium dioxide (TiO_2) nanoparticles with an average particle size of 10 - 15 nm in a water-based drilling mud system. The nanocomposite was added at concentrations of 0.3 to 3.7 wt%. The results indicated significant reductions in the filtration volume and filter cake thickness of a maximum of 64% and 65%, respectively, from the addition of 3.7 wt% of nanocomposite. Barry et al., 2015, conducted experiments evaluating the effect of the addition of iron oxide nanoparticle on the filtration properties of water-based muds. Iron oxide nanoparticles with two different particle sizes of 3 and 30 nm were added to a sodium-bentonite mud at a concentration of 0.5 wt%. The experiments were conducted at ambient and at high pressure-high temperature conditions (HPHT) conditions. The results demonstrated slight increases of 11 and 2% in the filtration volume from the addition of both 3nm and 30nm iron oxide particles, respectively, at ambient condition. However, more significant reductions of 28% and 23% were observed from the respective nanoparticles at HPHT condition. The high temperature of 200°C caused the sodium cations on the basal surface of the bentonite clay minerals to dissociate resulting in the substantial increase on filtrations of the base mud. The presence of iron oxide nanoparticles replaced the dissociated cations allowing the bentonite to be deflocculated, hence resulting in the significant reduction of the filtration volume. Results obtained by Bayat[b] et al., 2019, observed a slight reduction in the filtrate volume from water-based mud samples containing nanoparticles after being hot rolled at 50°C. Reductions of up to 14, 11, and 9% were indicated from the water-based mud samples containing 0.5 wt% of zinc oxide, titanium oxide, and silica nanoparticles, respectively

With all the research conducted in the past, however, investigations on the nano-based drilling muds in the low temperature conditions are still limited. On that basis, this research aims to investigate the role of nanoparticles as an alternative material in the formulations of thermally stable drilling muds in the aqueous-based system not only for the use in the high temperature but also low in the temperature conditions as encountered in the offshore deepwater and Arctic drilling operations.

METHODOLOGY

Materials and Mud Formulations

Drilling mud samples investigated in this research were focused on the aqueous-based mud systems consisting of the freshwater-based and the saltwater-based muds. Mud samples were prepared using additives commonly used in the oil industry, as presented in Table 1. The density of each component was obtained from the safety data sheet of each material.

Table 1 List of materials used in the preparation of drilling mud samples

Material	Function	ρ (kg/m^3)
Bentonite (Wyoming)	Primary viscosity, filtration control	2500
Bentonite (Cebogel)	Primary viscosity, filtration control	2300
Polyanionic cellulose (PAC-R)	Filtration control	1550
Xanthan gum (Barazan)	Viscosity, filtration control	1600
Barite (barium sulphate)	Weighting agent	4230
Caustic soda (Sodium hydroxide)	Alkalinity control	2130
Sodium chloride (NaCl)	Salt	2170
Potassium chloride (KCl)	Salt	1984
Calcium chloride (CaCl$_2$)	Salt	2150
Silica (SiO$_2$) nanoparticle	Potential additive	2300
Alumina (Al$_2$O$_3$) nanoparticle	Potential additive	3700

The mud samples were prepared by mixing all the components with their continuous phase fluids using a high-speed mixer. Concentration and mixing order of each component was carried out following the procedure recommended by Pabley, 1985. Distilled water was used as the continuous phase fluid in the freshwater-based mud system. Meanwhile, for the saltwater-based muds, a simplified artificial seawater was prepared as the continuous phase of fluid by dissolving *NaCl* (1.435 wt%), *KCl* (0.595 wt%), and *CaCl$_2$* (1.47 wt%) in a distilled water making up a salinity level of 35,000 ppm which represents the average salinity of seawater (Dickson and Goyet, 1994). Meanwhile, nanoparticles used in this research were silica and alumina nanoparticles with average particle diameters of 7 and 5 nm, respectively, and were added at various concentrations into the tested mud samples. Formulations of the tested mud samples are presented in Table 2.

Table 2 Formulations of the drilling mud samples

Mud Label	Water / Brine (ml)	Salinity (x1000ppm)	Bentonite (gr)	Caustic Soda (NaOH)	Xanthan Gum (gr)	Polyanionic Cellulose	Barite (gr)	NP Type	NP Concentration (gr)	NP Concentration (wt%)
Mud-1 (freshwater-based)	350	-	20	0.1	1	1	10	-	0.0	0
Mud-1+0.05wt% Silica NP	350	-	20	0.1	1	1	10	Silica 7nm	0.2	0.05
Mud-1+0.1wt% Silica NP	350	-	20	0.1	1	1	10	Silica 7nm	0.4	0.1
Mud-1+0.15wt% Silica NP	350	-	20	0.1	1	1	10	Silica 7nm	0.6	0.15
Mud-1+0.2wt% Silica NP	350	-	20	0.1	1	1	10	Silica 7nm	0.8	0.2
Mud-1+0.5wt% Silica NP	350	-	20	0.1	1	1	10	Silica 7nm	1.9	0.5
Mud-1+0.8wt% Silica NP	350	-	20	0.1	1	1	10	Silica 7nm	3.1	0.8
Mud-1+1wt% Silica NP	350	-	20	0.1	1	1	10	Silica 7nm	3.9	1
Mud-1+0.05wt% Alumina NP	350	-	20	0.1	1	1	10	Alumina 5nm	0.2	0.05
Mud-1+0.1wt% Alumina NP	350	-	20	0.1	1	1	10	Alumina 5nm	0.4	0.1
Mud-1+0.15wt% Alumina NP	350	-	20	0.1	1	1	10	Alumina 5nm	0.6	0.15
Mud-1+0.2wt% Alumina NP	350	-	20	0.1	1	1	10	Alumina 5nm	0.8	0.2
Mud-2 (saltwater-based)	350	35	20	0.1	1	1	10	-	0.0	0
Mud-2+0.05wt% Silica NP	350	35	20	0.1	1	1	10	Silica 7nm	0.2	0.05
Mud-2+0.1wt% Silica NP	350	35	20	0.1	1	1	10	Silica 7nm	0.4	0.1
Mud-2+0.15wt% Silica NP	350	35	20	0.1	1	1	10	Silica 7nm	0.6	0.15
Mud-2+0.2wt% Silica NP	350	35	20	0.1	1	1	10	Silica 7nm	0.8	0.2
Mud-2+0.5wt% Silica NP	350	35	20	0.1	1	1	10	Silica 7nm	1.9	0.5
Mud-2+0.8wt% Silica NP	350	35	20	0.1	1	1	10	Silica 7nm	3.1	0.8
Mud-2+1wt% Silica NP	350	35	20	0.1	1	1	10	Silica 7nm	3.9	1
Mud-2+0.05wt% Alumina NP	350	35	20	0.1	1	1	10	Alumina 5nm	0.2	0.05
Mud-2+0.1wt% Alumina NP	350	35	20	0.1	1	1	10	Alumina 5nm	0.4	0.1
Mud-2+0.15wt% Alumina NP	350	35	20	0.1	1	1	10	Alumina 5nm	0.6	0.15
Mud-2+0.2wt% Alumina NP	350	35	20	0.1	1	1	10	Alumina 5nm	0.8	0.2

Rheological Properties Evaluation

This investigation was conducted to evaluate the rheological properties of drilling muds through a direct measurement obtained from a rotational viscometer. The experiments were carried out in compliance with the API Recommended Practice 13B as the standard for drilling muds testing procedure. The viscometer was used to measure the shear rate and shear stress at different rotational speeds. The recorded data were then used to determine rheological properties based on the Bingham plastic model. The evaluated properties are plastic viscosity, yield point and gel strengths, calculated using the following formulas.

$$\mu_B = DR_{600} - DR_{300} \qquad (1)$$
$$\tau_y = 0.48 \times (DR_{300} - \mu_B) \qquad (2)$$
$$GS = 0.48 \times DR_3 \qquad (3)$$

In which DR_{600}, DR_{300}, and DR_3 are the dial readings at 600, 300 and 3 RPM, respectively, whilst μ_B, τ_y, and GS are the Bingham plastic viscosity *(mPa.s)*, yield point *(Pa)*, and gel

strength *(Pa),* respectively. To simulate temperature conditions in Arctic drilling, the mud samples were tested at temperatures between 0 and 80°C. For this purpose, a cooling device was designed to accommodate measurements below ambient temperature. The new device was technically a hollow-walled cooling cup connected to a refrigerating bath circulating cooling fluid through the cup wall and bringing the temperature of the mud sample down. Figure 1 shows the simplified diagram of the cooling cup and its positioning alongside the viscometer.
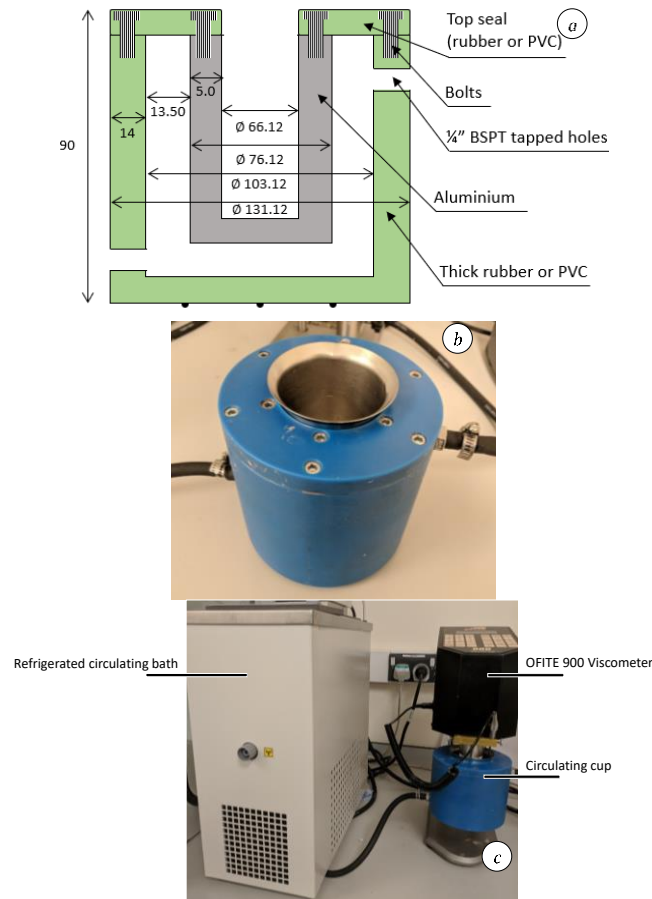
Figure 1 (a) schematic diagram (in mm), (b) actual view, and (c) positioning of the newly designed cooling cup

Filtration Properties Evaluation

The experiments were conducted using a standard API Filter Press to evaluate static filtration properties of drilling mud at room temperature and under 700 kPa (100 psi) differential pressure for 30 minutes, after which the accumulated filtrate volume was recorded and the thickness of the recovered filter cake was measured. Spurt loss volume and filtration rate were also calculated to analyse the impact of nanoparticles on the filtration properties of the mud samples.

RHEOLOGICAL PROPERTIES RESULTS

Silica-Added Muds

Freshwater-based muds

Rheological properties of the freshwater-based mud samples containing silica nanoparticles measured at ambient temperature condition (20°C) are illustrated in Figure 2. The results showed a significant reduction on the overall rheological properties from the addition of silica

nanoparticles. Biggest reductions of up to 34% and 32% were observed on the plastic viscosity and yield point at silica concentrations of 1 and 0.8 wt%, respectively (Figure 2a). Meanwhile, silica concentrations of 0.05wt% demonstrated the biggest drop on 10-second and 10-minute gel strengths, at about 46% and 50%, respectively (Figure 2b). The thinning effect with the increasing concentration of silica was caused by a combination of the high repulsion force between the silica nanoparticles and the clay minerals, as well as the reduced hydrogen bonding between silica and polymers caused by the high ionisation of silica in high pH solutions.
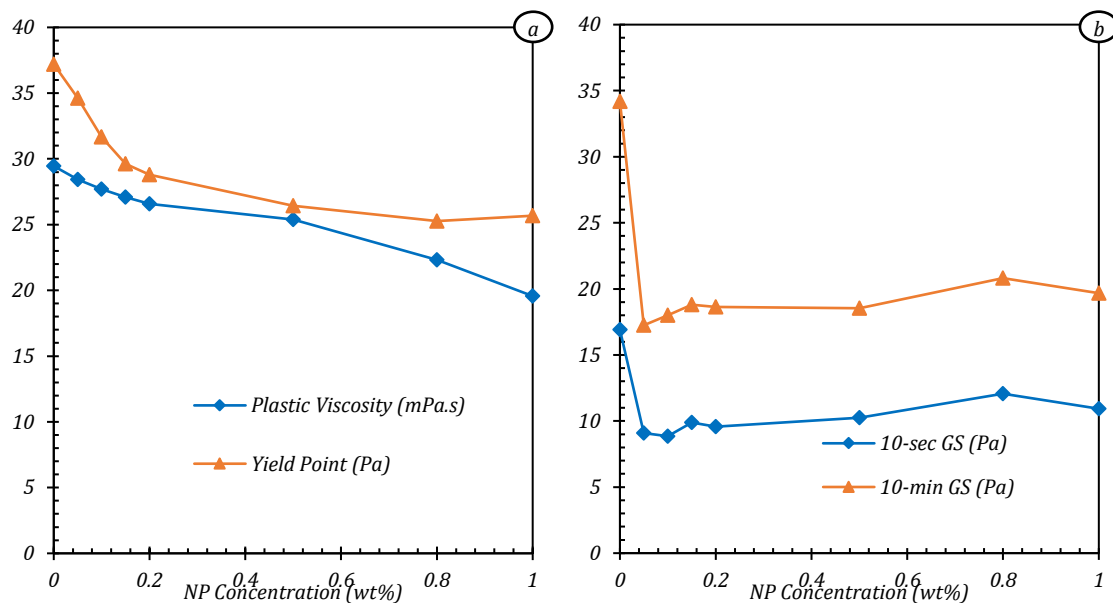
Figure 2 (a) plastic viscosity, yield point, and (b) gel strengths of the freshwater-based muds containing various concentrations of silica nanoparticles

Reactive clay materials such as montmorillonite in bentonite exhibits a permanently negative charge on its basal surface layers and a pH-dependent surface charge on the edges of clay platelets. The edge of the platelet will typically be protonated exhibiting a more positively charged surfaces (Figure 3) (Tournassat et al., 2013, 2015). At the same time, silica also exhibits a highly negative charge on the surface of the particles when dispersed in a polar medium such as water. Metin et al., 2011, observed an electrostatic potential of up to -50 mV from the suspension of silica at 0.5 wt% concentration with an average particle diameter of 25 nm. When it is added to a bentonite suspension, the highly negative surface charges between the two materials increase the interparticle repulsive forces resulting in the higher degree of dispersion manifested by the reduction in the mud physical properties.
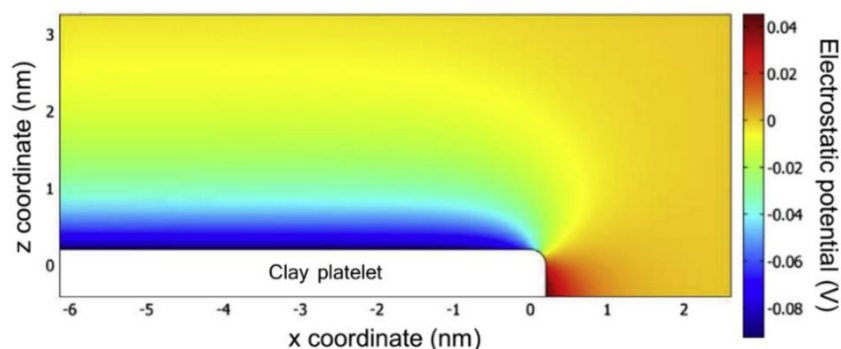

Figure 3 Electrostatic potential charge distribution on the surfaces of clay platelet: negatively charged basal surface and positively charge edge surface (adapted from Tournassat et al., 2015)

The interaction between silica particles and dispersible polymers such as xanthan gum also contributes to the higher degree of dispersion of the mud colloidal suspension. The interaction occurs through a hydrogen bonding between the hydroxyl $(-OH)$ groups of the particle surfaces and polymer molecules at pH levels below 3 (Oh et al., 1999b). However, when dispersed in aqueous medium at high pH, as it is the case with the mud samples, the silanol groups $(-SiOH)$ of the silica are ionised easily to become $-SiO^-$, resulting in the highly negative surface charged of particles. As a consequence, this ionisation process eliminates the number of the hydroxyl groups ready for hydrogen bonding with the polymer molecules (Katiyar and Singh, 2018), hence the reduction on the mud physical properties was observed from the experimental results.

As the silica concentrations increases, the reduction rate became smaller up to a point at which an increasing trend started to develop. This phenomenon was clearly indicated particularly from the yield point and the gel strengths results. A rise on the yield point from 25.3 to 25.7 Pa was observed at silica concentrations between 0.8 and 1 wt%, respectively (Figure 2a). Meanwhile, an increase in the gel strengths was observed at a smaller concentration of 0.1 wt% following the sharp drops from the base value (Figure 2b).

As well as the evaluations at ambient temperature condition, the mud samples were also evaluated at temperatures between 0 and 80°C. Figure 4 illustrates the rheological properties results at 0-80°C. As shown in Figure 4a, the base sample (Mud-1) exhibited a decreasing trend on plastic viscosity as the temperature increases, with the highest of 48.4 mPa.s was recorded at 0°C and down to just 12.7 mPa.s at 80°C, a reduction of about 74%. The thinning behaviour was simply caused by the reduction of the water viscosity with the increasing temperature resulting in the decreasing profile of the mud physical property at high shear rates (Caenn et al., 2017b; Hilfiger et al., 2016). The similar trend was also observed from the yield point results in Figure 4b, in which a reduction of 49% was recorded from 51.3 Pa to 26.1 Pa as observed at 0 and 80°C, respectively.

With the addition of silica nanoparticles, the mud samples indicated an increase of thermal stability as reflected from the smaller disparity between properties measured at 0 and 80°C. For instance, the sample containing 0.1 wt% silica nanoparticle observed plastic viscosities of 38.8 and 19.4 mPa.s corresponding to a 20% reduction and an increase of 53.5% at 0 and 80°C, respectively. Meanwhile, yield points were observed at 43.2 and 24 Pa corresponding to reductions of 15.8% and 8.9% at the respective temperatures . The improved stability on plastic viscosity and yield point was obtained due to the fact that silica is a ceramic material that is thermally resistant, contributing to a more stable profile across the temperature range (Adair et al., 2001; Medhi et al., 2020). A low and more constant plastic viscosity is desirable when drilling through formations with vast temperature difference, such as Arctic condition. A mud with low plastic viscosity will provide the higher jet velocity of the bit nozzle, resulting in a higher drilling rate of penetration. Besides, the more stable profiles of plastic viscosity over the broad temperature conditions will be beneficial in maintaining constant equivalent circulating density (ECD). If plastic viscosity is the measure of the resistance to flow at high shear rates, then the yield point is the measure of the initial resistance to flow of the muds. It reflects the interaction forces between particles at low shear rates, in which the tendency of the colloidal particles to link and bond together is higher than at high shear rates. In the field, it is used as

an annular flow indicator and a parameter for a good carrying capacity of the drilling muds. A high yield point is more favourable as the mud is more likely to have a better cutting carrying capacity, however, an excessive yield point is always avoided as it increases the pump power required to start a flow (Caenn et al., 2017b).

The increased stability was also reflected from the gel strength results as shown in Figure 4c and d. As shown, the base sample (Mud-1) already demonstrated a relatively constant profile on the 10-second gel strengths across the temperatures with an average of 17.2 Pa, as shown in Figure 4c. Meanwhile, the 10-minute gel strengths fluctuated slightly with the highest of 35.8 Pa recorded at 60°C, as presented in Figure 4d. The big difference between the two gel strengths indicates a progressive rate of gelation developed over time. With the addition of silica nanoparticle, a more flattened curve was observed on both 10-second and 10-minute gel strengths, indicating the improved thermal stability across the observed temperature conditions. Moreover, the smaller gap between the two gels also indicates a lower rate of gelation over time. Mud sample containing 0.1 wt% silica (diamond-shaped data points) provided the most stable profiles with an average of 9.1 and 15.6 Pa for 10-second and 10-minute gels, respectively.
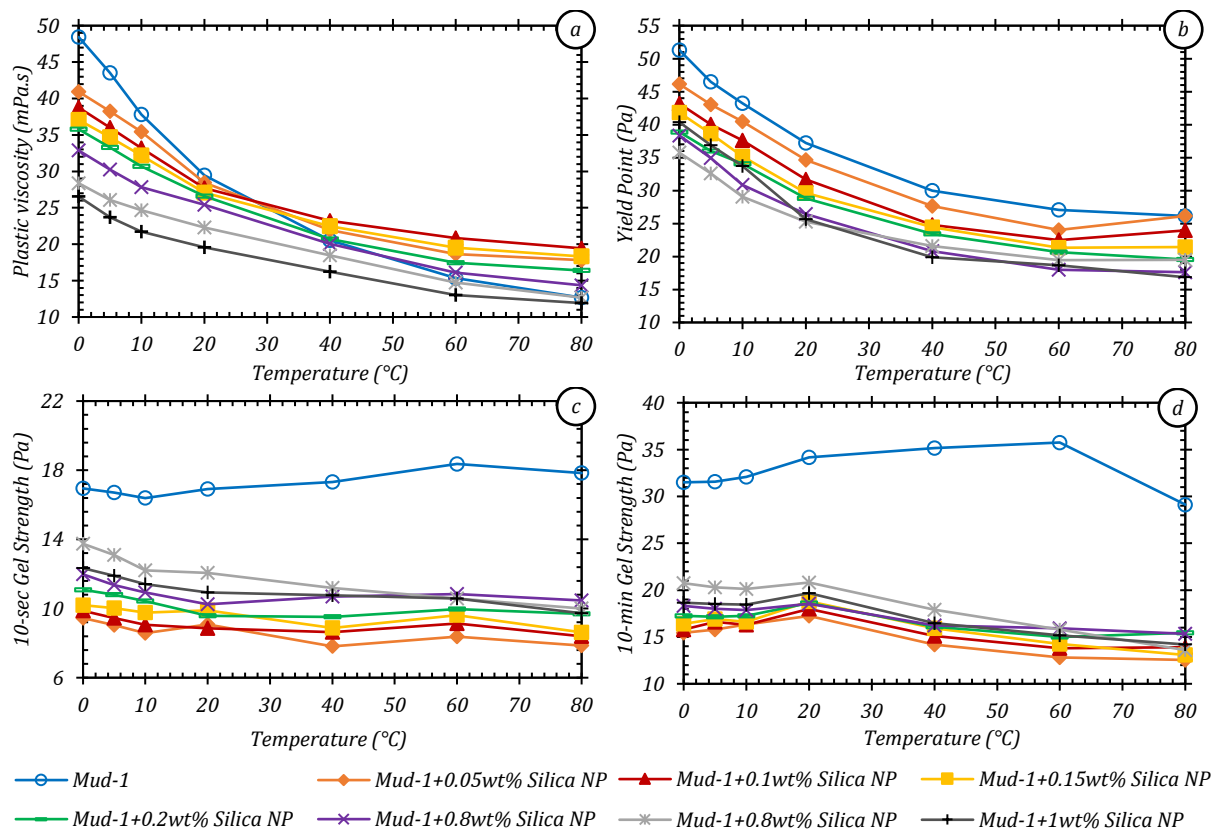

Figure 4 Results of the (a) plastic viscosity, (b) yield point, and (c) the 10-second and (d) 10-minute gel strengths of the freshwater-based muds containing various concentrations of silica nanoparticle over temperature range between 0 and 80°C

Like the yield point, gel strengths also indicate the strength of the attractive forces between particles under static conditions. They reflect the thixotropic behaviour of the drilling muds when the circulation is ceased for some time (Caenn et al., 2017b). In the field, they represent the shear stress required to breakdown the gel structure of the mud to restart the flow. They are

also an indicator of the ability of the mud to suspend cutting and weighting material within the mud column. Machado and Aragao, 1990, suggested that a gel strength of about 5 Pa is sufficient to suspend cutting and provide good carrying capacity. Low and flat gels over time are always favourable as they indicate a constant rate of gelation. Whilst high and excessive gel strengths are avoided as they can cause swab and surge issues as well as making the separation of cuttings and mud more difficult. The current results suggested that the addition of silica nanoparticle in the freshwater-based system can be beneficial in reducing gel strengths and exhibit a more constant profile throughout the temperature conditions.

Saltwater-based muds

Figure 5 presents the results on the rheological properties of the saltwater-based mud samples containing various concentrations of silica nanoparticle at ambient temperature condition. Significant reduction in rheological properties was observed from the presence of salt ions as indicated from the base sample without the addition of nanoparticles. In the absence of silica nanoparticles, plastic viscosity decreased significantly about 54% from 29.5 mPa.s, as obtained from the freshwater mud, to 13.6 mPa.s at 0% silica concentration shown in Figure 5a. Yield point also showed a decrease of about 70% from 37.2 Pa in the freshwater mud to 11.3 Pa in the saltwater-based mud. Meanwhile, gel strengths were contracted significantly about 84% from 16.9 to 2.7 Pa on the 10-second gel and about 91% from 34.2 to 3 Pa on the 10-minute gel (Figure 5b). The swelling mechanism of clay minerals occurs from the adsorption of water molecules on to the basal surfaces of the clay platelets, allowing the hydration and expansion of the lattice structure of the clay minerals. Hence, providing consistency and volume increase of the mud colloidal suspension (Norrish, 1954). When electrolytes are present in the bulk of the solution, cations are drawn on to the negatively charged clay surface layers. This will disrupt the hydrogen bonding by pushing away water molecules and attaching to the clay surfaces, lowering the swelling capacity of the clay minerals (Caenn et al., 2017c). Hence, causing the reduction on the physical properties of the base sample of the salt muds.

On the other hand, the addition of silica nanoparticle to the salt-based muds had resulted in a decreasing trend on the plastic viscosity with the increasing concentration up to 0.2 wt%, in which the mud sample indicated a reduction of up to 18.5%. As discussed earlier that particle interactions are affected by the distance between particles. The closer distance between two particles the greater the tendency to attract each other and to flocculate. However, particles with highly negative surface charge will exhibit a stronger repulsion when they are close to each other up to a point when attraction force grows more dominant as a consequence of the higher particle collision due to stronger Brownian motion as the concentration increases (Wang et al., 2012; Yapici et al., 2018). This explains the slight reduction in the plastic viscosity observed from the results at the lower silica concentrations below 0.2 wt%. Beyond this concentration, plastic viscosity was observed to slowly improve with the final improvement of 8.5% observed at the concentration of 1 wt%, as indicated in Figure 5a. The growing of the attractive force is more clearly observed from the low shear rate properties indicated from the yield point results. A small increase of 3.7% was already observed from the silica concentration of 0.05 wt% and the increasing trend continues steadily with the final increase of 23.5% observed at 1 wt% silica. Results on gel strengths were also indicating the higher degree of flocculation attribute from the growing of attraction between particles. A significant rise of up

to 118% was observed at the concentration of 0.2 wt%, beyond which a more stable profile was obtained with the increasing silica concentration (Figure 5b). The addition of silica also resulted in a more stable gelation rate indicated from the narrow gap between the 10-second and 10-minute gel profiles across the overall concentrations. The higher flocculation degree was caused by the presence of electrolytes in the mud colloidal suspension. Additional cations tend to be attracted and adsorbed on to the surfaces of silica particles, compressing the electrical double layer, thus reduces particle repulsion forces (Metin et al., 2011; Oh et al., 1999a).
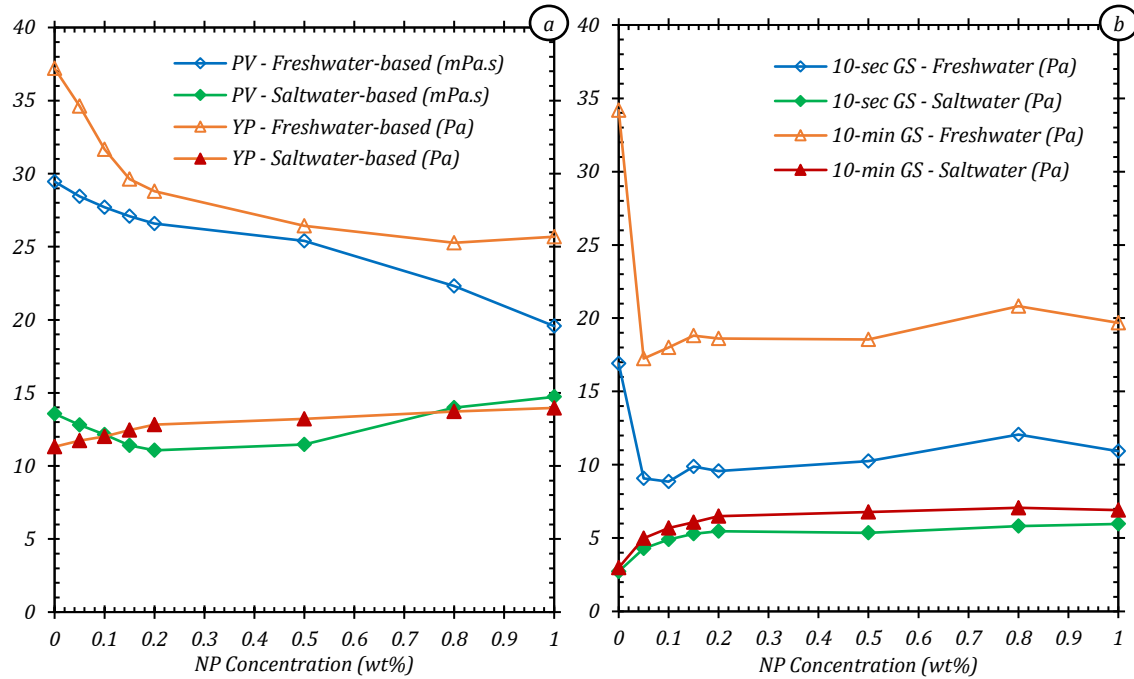
Figure 5 Results of the (a) plastic viscosity, yield point, and (b) gel strengths of the saltwater-based mud samples containing various concentrations of silica nanoparticles

Figure 6 presents the results on the rheological properties of the saltwater-based muds at low and high temperatures. As shown, the base sample (Mud-2) exhibited a temperature-dependent behaviour indicated from the decreasing profile on plastic viscosity with the increasing of temperature (Figure 6a). A significant reduction of more than 75% on plastic viscosity was observed from 20.8 to 5.1 mPa.s measured at 0°C and 80°C, respectively. Meanwhile, a 74% reduction was observed on the yield point from 17.7 to 4.6 Pa across the temperature range. With the addition of silica nanoparticles, an increasing trend was observed on both plastic viscosity and yield point. Especially at elevated temperature conditions (>20°C), higher degree of flocculation was attributed to the higher chance of collision between particles as a result of the increased kinetic energy of the system and stronger Brownian motion as the temperature continued rising (Metin et al., 2011; Omurlu et al., 2016). On the other hand, as the effect of the low-temperature condition (<20°C) was lessened due to the presence of salt ions lowering the freezing point of water, the addition of silica nanoparticles exhibited a more constant profile due to the more stable colloidal suspension resulted from the maintained stronger repulsion between particles (Vargas et al., 2019). The improved thermal stability was reflected from the plastic viscosity and yield point profiles with the optimum range observed from the sample containing 0.1 wt% of silica, as indicated from the diamond-shaped data points in Figure 6. At 0°C, plastic viscosity was recorded at 12.9 mPa.s, a reduction of 38% from 20.8 mPa.s (Mud-

2), whilst at 80°C viscosity was at 8.4 mPa.s, a 65% increase from 5.1 mPa.s (Figure 6a). Yield points were observed in between 12.7 Pa, corresponds to 28% reduction from 17.7 Pa (Mud-2) at 0°C, and 8.8 Pa, a 92% increase from 4.6 Pa at 80°C (Figure 6b).

The constant rheological profiles were also reflected from the results on the gel strengths as presented in Figure 6c and d. The base sample (Mud-2) indicated a fairly low and constant rate of gelation indicated from the stable curves of gel strengths over time across the temperature range. At 0°C, the 10-second and 10-minute gels were observed at 3.1 and 3.5 Pa (Figure 6c and d, respectively), whilst at 80°C, both gels were observed at a constant value of 1.9 Pa. The addition of silica increased both gel strengths significantly with the retained constant profiles across the temperature range as the nanoparticle concentration increases. Mud sample containing 0.1 wt% silica indicated the most favourable results with 10-second and 10-minute gels at 0°C between 5.4 and 6.4 Pa, respectively, and stabilised throughout the temperature conditions with 5.6 and 6.1Pa were observed at 80°C for the respective gelation times. As discussed in the earlier, the presence of salt ions suppresses the electrostatic potential of the particles from the adsorption of cations on to the particle surfaces. Consequently, the repulsion force is reduced resulting in the more dominant attraction between particles increasing the degree of flocculation, hence increasing low shear rate properties of mud suspension (Adair et al., 2001; Metin et al., 2011; Oh et al., 1999a).
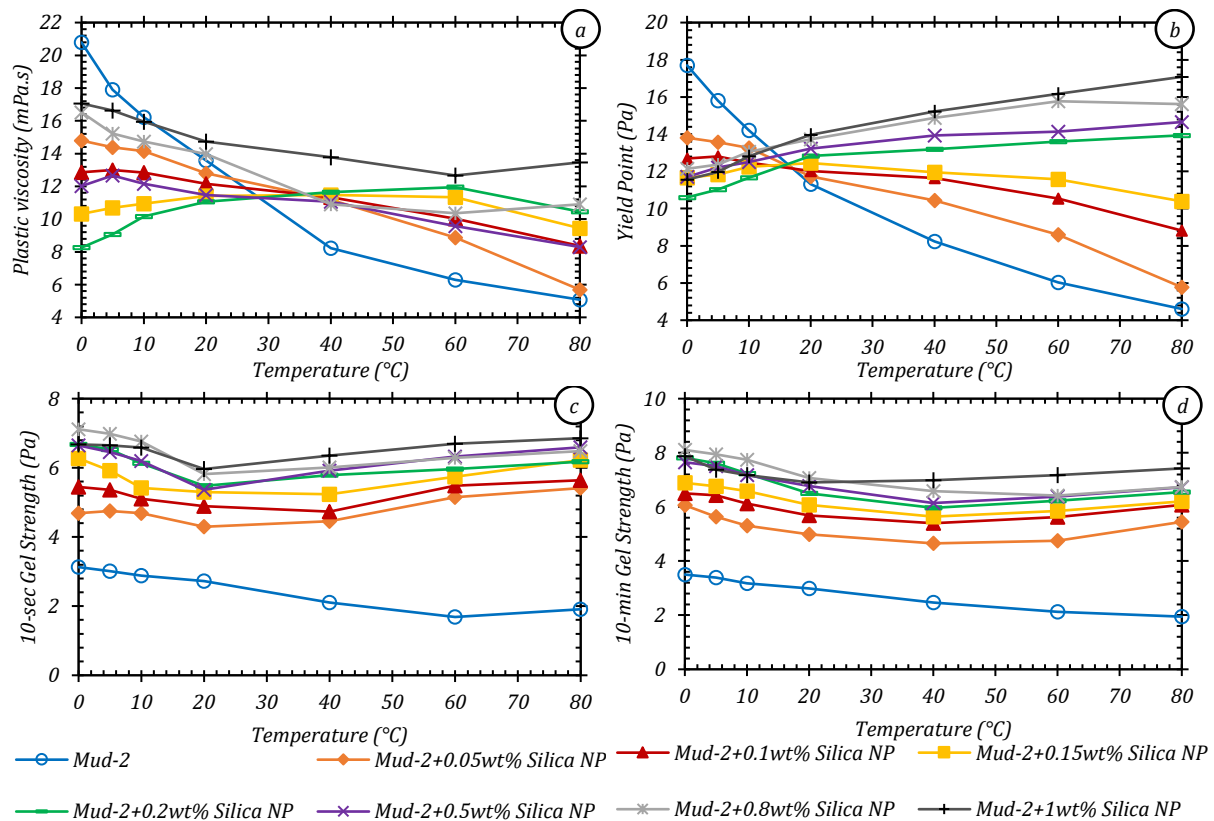

Figure 6 Results of the (a) plastic viscosity, (b) yield point, and (c) the 10-second and (d) 10-minute gel strengths of the saltwater-based muds containing various concentrations of silica nanoparticle over temperature range between 0 and 80°C

Although there are still very few studies conducted in the past investigating the performance of silica-added muds under both low and high temperatures, studies conducted by Taraghikhah et al., 2015, and Medhi et al., 2020, might provide a comparison to what have been observed

in the current study. Summary of their results on the plastic viscosity is presented Figure 7 alongside the results from the current study. The graph presents plastic viscosity results from the addition of 0.5wt% of silica nanoparticles in the aqueous-based mud systems. In their experiments, Taraghikhah et al. added 0.5 wt% silica with 1-60 nm particle diameter to a mud containing certain amounts of salts, viscosities, and filtration control polymers, although they did not specify the quantity of each component in their report. Meanwhile, Medhi et al. added silica with a particle diameter of 22-48 nm to a mud containing sodium chloride, soda ash, biocide, and various types of polymers. As shown, the result observed from Taraghikhah et al.'s sample indicated a similar trend to the results obtained from the current study (Muds-7 and 10), as a reduction of 13% on plastic viscosity was recorded at ambient temperature from the addition of silica. An increase of 38% was observed after the mud sample was hot rolled at 120°C. Meanwhile, Medhi's results demonstrated a very high plastic viscosity up to 64 mPa.s after hot roll at 80°C from the addition of 0.5 wt% silica. The high physical properties observed from Medhi's results could have been caused by the use of various types of polymers in the mud formulation.
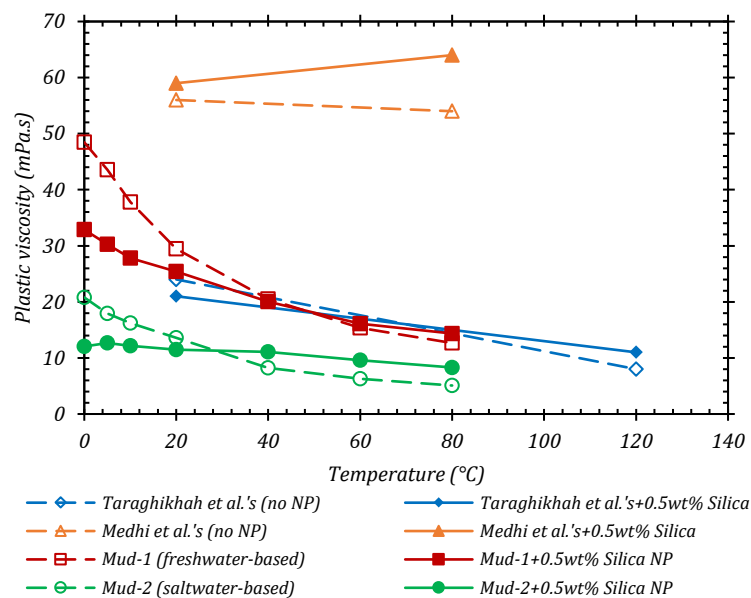

Figure 7 Results of the plastic viscosity of the water-based muds containing 0.5wt% of silica nanoparticle from the current and past studies (Medhi et al., 2020; Taraghikhah et al., 2015)

As discussed earlier, the presence of high molecular weight of polymers will increase mud physical properties due to their ability to bridge and crosslink solid particles within the mud suspension (Caenn et al., 2017a). Alteration magnitudes of drilling mud properties from the addition of silica nanoparticles are very much affected by the types and concentrations of other components present in the mud suspension. For instance, the presence of high molecular weight long-chained substances, or the presence of strong electrolytes will affect the interaction between silica and other electrostatically charged particles (Adair et al., 2001; Oh et al., 1999a, 1999b; Wang et al., 2012). Trends from the past researchers concluded that the addition of small quantities (<1 wt%) of unmodified silica nanoparticles would typically decrease physical properties of muds with simple compositions (e.g. clay minerals, one or two types of polymers, monovalent salt cations), thus adding higher concentrations or pre-treating the silica nanoparticle are required to observe an increase on the mud physical properties (Hassani et al.,

2016; Jain et al., 2015; Mao et al., 2015; Medhi et al., 2020; Srivatsa and Ziaja, 2012; Taraghikhah et al., 2015). In this research, a silica concentration threshold of 0.8 wt% was observed, above which the mud physical properties started to increase.

Alumina-Added Muds

Alumina is the most widely produced oxide ceramic material with widespread use in various applications from engineering through biomedical (Ben-Nissan et al., 2008). However, further studies are still needed to be conducted, especially evaluating the role of alumina nanoparticle in the alteration of drilling mud properties. For that purpose, alumina with an average particle diameter of 5 nm was used in this study, added to both freshwater and salt-based mud systems at particle concentrations between 0.05 and 0.2 wt%. The freshwater-based system was prepared the similar way as the previous silica-added muds using distilled water as the continuous phase, whilst the brine with 35,000 ppm salinity was used in the preparation of the saltwater-based mud system.

<u>**Freshwater-based muds**</u>

Figure 8 presents the rheological properties of the freshwater-based muds containing alumina nanoparticles at the ambient temperature condition. As shown in Figure 8a and b, significant increases were observed on both the plastic viscosity and the yield point of up to 70.2% and 23.8%, respectively, at the concentration of 0.2 wt%. The results on gel strengths also showed an increasing trend with the increasing concentrations of alumina nanoparticles, as presented in Figure 8c and d. Improvements of up to 44.3% and 18.6% were observed on the 10-second and 10-minute gels, respectively, from the sample containing 0.2 wt% of alumina nanoparticle. These results indicate an opposite trend when compared to the results observed from muds containing silica in which the rheological properties were decreased with the addition of silica nanoparticles. This was caused by the different types of electrostatic charge on the surface particles of silica and alumina when dispersed in water. Although both are ceramic materials, silica and alumina have different isoelectric points (IEP) or point of zero charges (PZC), which defined as the pH level at which particles are charged neutral. For silica, it is around pH 1.5-3.7, whilst for alumina, it is 7-9 (Adair et al., 2001). These PZC define the magnitudes of the surface charges of the dispersed particles. At pH levels below the PZC, particles will exhibit a positive charge and will be negative at pH levels above the PZC. Increases of magnitudes, whether positive or negative, occur as the pH levels further away from the PZC, resulting in the more dominant electrostatic repulsive force of particles, causing the higher degree of dispersion. Meanwhile, smaller magnitudes occur at pH levels near the PZC resulting in the more dominant van der Waals attraction force that will increase the tendency of particles to flocculate. Unlike silica, alumina nanoparticle exhibits positively charged particles when dispersed in an aqueous medium at neutral pH value. Patel et al., 2015, measured the zeta potential of the suspensions of alumina and silica nanoparticle. The results observed a positively charged alumina suspension of +20 mV as opposed to -30 mV obtained from silica with the same particle concentration. However, the zeta potentials decreased with the increasing pH levels due to the deprotonation of the particle surfaces, and at pH 11, zeta potentials of -15 mV and -50 mV were observed from alumina and silica, respectively (Adair et al., 2001; Patel et al., 2015). Zeta potential is a measure to determine the surface charge of particles in colloidal suspension. Dispersions with zeta potentials lower than +25 or higher than

-25 are classified as to have a high degree of flocculation due to the stronger attractive force between particles. Meanwhile, suspensions with greater absolute charges will exhibit increasing stability of particle dispersion attributed to the higher repulsive force (Kumar and Dixit, 2017). Therefore, the increase in the physical properties of the alumina muds observed from the experiments was caused by the higher tendency of flocculation attributed to the stronger interparticle attractive forces.
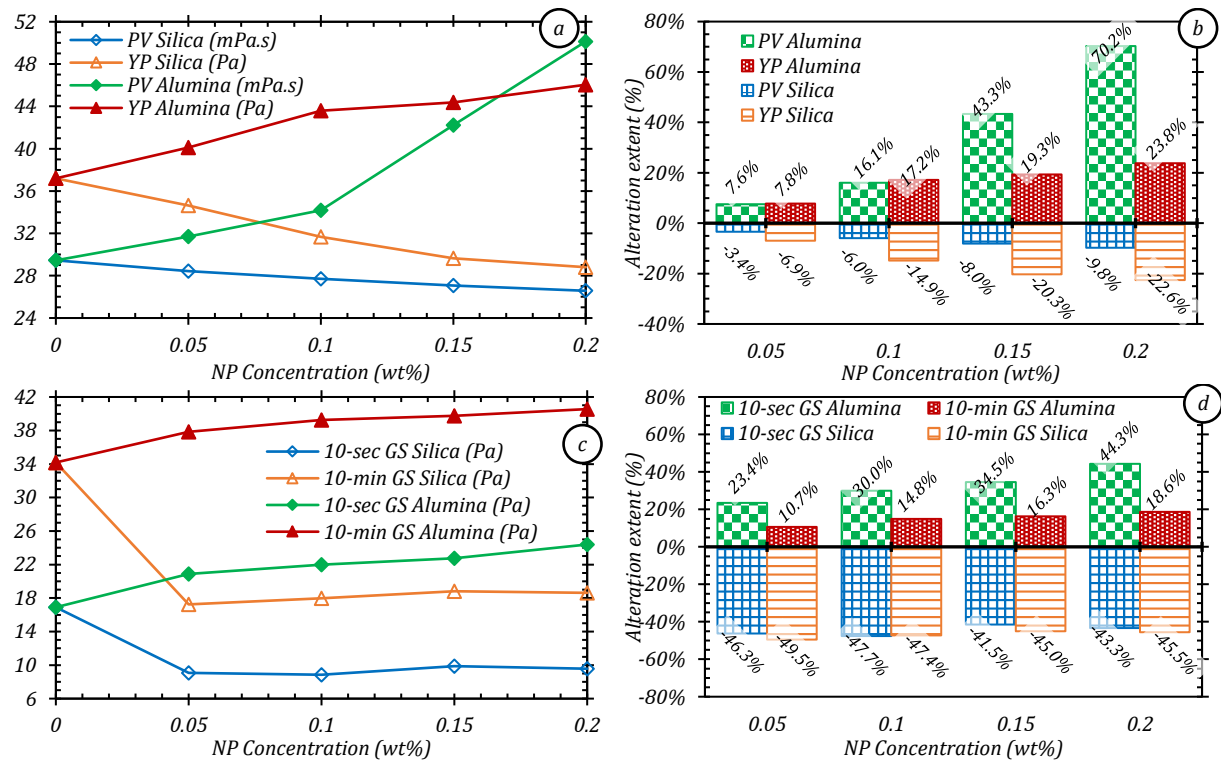

Figure 8 Rheological properties profiles (a and c) and alteration extents (b and d) of the freshwater-based muds containing alumina nanoparticles compared to those containing silica nanoparticles

Results of the rheological properties evaluation at low and high temperature conditions are illustrated in Figure 9. As the base sample (Mud-1) presented in the graph was the same reference sample used in the silica evaluation, it can be recalled that the decreasing trend on the plastic viscosity and yield point shown in Figure 9a and b, respectively, was caused by the reduction of water viscosity across the temperature range (Caenn et al., 2017b; Hilfiger et al., 2016). The addition of alumina nanoparticles exhibited an increased thermal stability as indicated from the more stable curves of plastic viscosity and yield profiles across the temperature range. This was indicated from the smaller differences between results at 0 and 80°C. For instance, the sample containing 0.05 wt% of alumina exhibited a viscosity of 40 mPa.s at 0°C, a 17.3% reduction from the base sample, whilst 25.1 mPa.s was observed at 80°C which corresponding to a 98% increase. Meanwhile, the yield points were recorded at 45.7 and 34.2 Pa, corresponding to a 10.9% reduction and a 30.9% increase at 0 and 80°C, respectively. The more stable profiles of plastic viscosity and yield point over the observed temperature range is attributed from the improved thermal stability of the mud samples with the addition of alumina nanoparticle. As a ceramic material, alumina is known to have a good heat resistance making it suitable to be used as an additive to maintain stable rheological properties, especially for application in extreme temperature conditions (Ivanov et al., 1999; Medhi et al., 2019).

Results on gel strengths also exhibited significant increases with the increasing concentration of alumina nanoparticles, as shown in Figure 9c and d. Sample containing 0.05 wt% of alumina showed an average increase of 21.5% on the 10-second gel and 21.6% on the 10-minute gel as compared to the results of Mud-1. Although, both gel strengths showed the indication of good thermal stability, the rate of gelation was also increased, which reflects the greater disparity between the 10-second and 10-minute gels. In the field, the higher rate of gelation might not be favourable as it is associated with higher pump power required to restart mud circulation after being ceased for some time. This might result in the sudden increase of annular circulating pressure which may cause well control problems, such as loss circulation or fracturing of the rock formations (Caenn et al., 2017d).
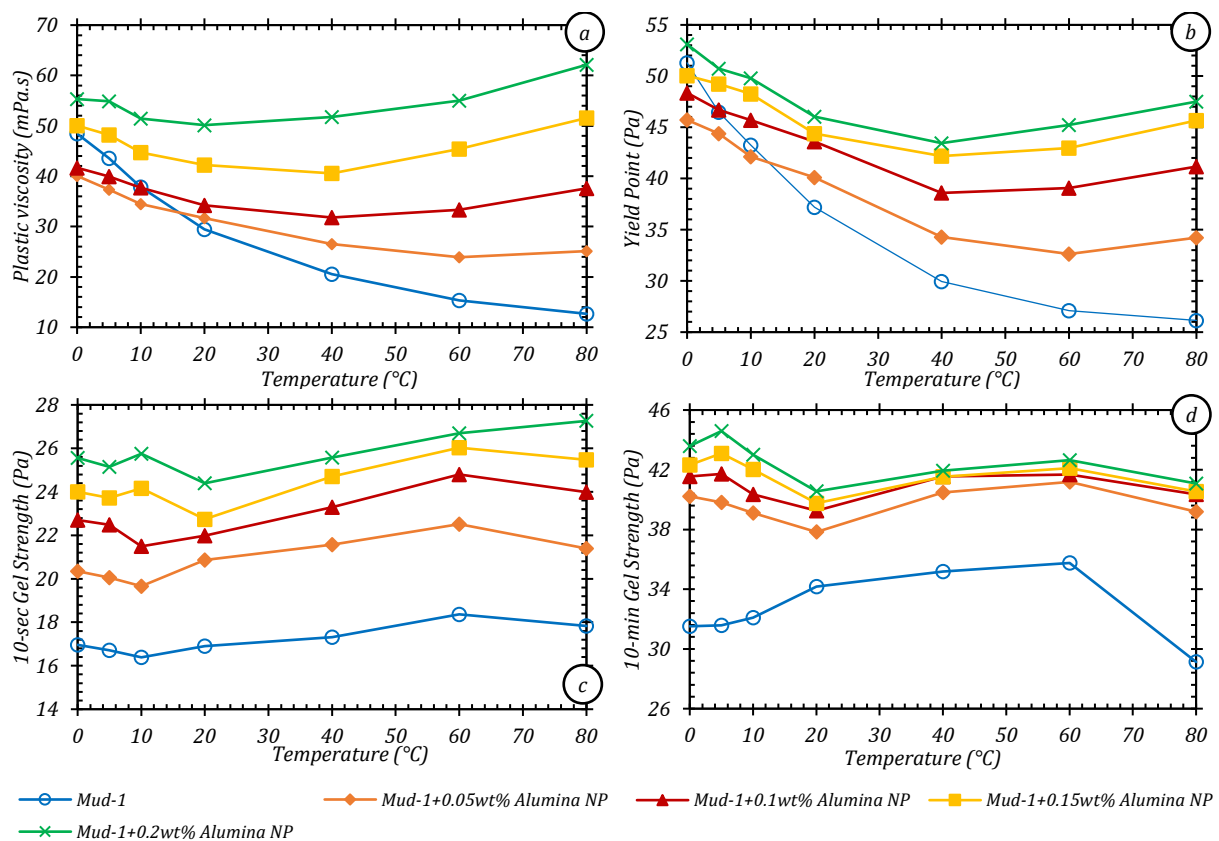

Figure 9 Results of the (a) plastic viscosity, (b) yield point, and (c) the 10-second and (d) 10-minute gel strengths of the freshwater-based muds containing various concentrations of alumina nanoparticle over temperature range between 0 and 80°C

Saltwater-based muds

Rheological properties results of the saltwater-based muds containing alumina are presented in Figure 10. As it was experienced with the silica muds, the addition of alumina showed a small reduction on plastic viscosity up to the concentration of 0.1 wt% where a reduction of 11% was observed (Figure 10a). The reduction was caused by the higher particle repulsion from the addition of low concentrations of alumina increasing the dispersion state of mud suspension when high shear rates are applied. As discussed earlier, electrostatic potential of alumina particle at high pH is slightly negative, resulting in an interparticle repulsion with the clay platelets. However, with the increasing concentrations, an increasing trend was observed with the final improvement of 2.5% was indicated from the sample containing 0.2 wt%. the increasing trend was attributed to the stronger particle attraction caused by the higher chance

of collision between particles from the stronger Brownian motion. Meanwhile, an increasing trend on the yield point was observed from the beginning of the addition of alumina nanoparticles, with up to 43% increase was recorded at the particle concentration of 0.2 wt% (Figure 10a). Both the 10-second and 10-minute gel strengths also gradually increased with the maximum improvements of 45% and 58%, respectively, observed at the concentration of 0.2 wt% (Figure 10b). The increasing trend of the low-shear rate properties manifested by the yield point and gel strengths with the increasing concentrations of alumina nanoparticles was caused by the higher degree of flocculation as the salt ions were adsorbed on to the basal surface clay platelets and also on the surface of alumina particles forcing the electric double layer to shrink (Çınar and Akinc, 2014; Jailani et al., 2008). The narrower gap between the two gel strengths as shown in Figure 10b also indicated a lower gelation rate across the overall concentrations. This is more desirable as the higher rate of gelation tends to produce an excessive gel strength when circulation is ceased for a longer time (Caenn et al., 2017b; Hilfiger et al., 2016).
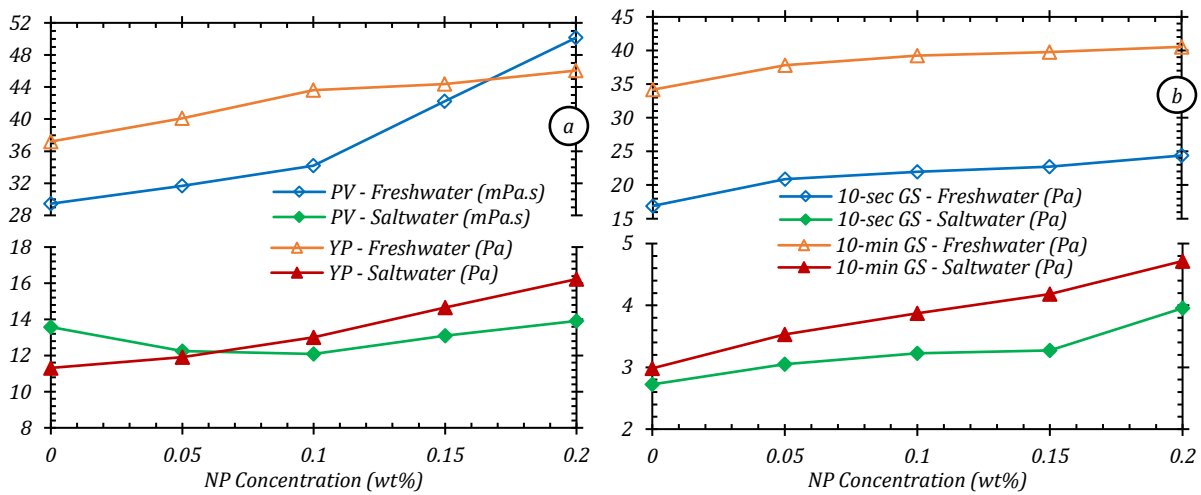

Figure 10 Results comparison on the plastic viscosity and yield point (a) and the 10-second and 10-minute gel strengths between the saltwater-based and freshwater-based muds containing various concentrations of alumina nanoparticles

For the rheological properties evaluation at low and high temperature conditions, Figure 11 presents the results of the mud samples containing alumina nanoparticles in the saltwater-based system. At conditions below ambient temperature (<20°C), significant reductions on plastic viscosity were observed with the increasing temperature across the nanoparticle concentrations, as shown in Figure 11a. The biggest reduction was observed from the sample containing 0.1 wt% of alumina at 0°C, with the measured plastic viscosity of 15.2 mPa.s, which corresponds to a reduction of 27% from 20.8 mPa.s as observed from the base sample (Mud-2). Meanwhile, at temperatures above 20°C, plastic viscosity indicated a rise as the concentration increases. The highest increase was observed from the sample containing 0.2 wt% of alumina at 80°C, with the measured viscosity of 8 mPa.s corresponding to a 57% increase from 5.1 mPa.s obtained from the base sample. Results on the yield point exhibited an improvement with the increasing concentration almost at the entire temperature range. Sample containing 0.2 wt% of alumina observed a yield point of 18.1 Pa, a slight improvement of 2.5% from 17.7 Pa as observed from the base sample at 0°C. Meanwhile, the biggest improvement of 117% increase was recorded from the same sample at 80°C, as shown in Figure 11b.

The presence of electrolytes shrinks the electric double layer of alumina particles as the cations are being adsorbed onto the particle surfaces. This produces stronger attractive forces between particles which promote a higher degree of flocculation increasing rheological properties of the mud samples. The higher degree of flocculation is also caused by the stronger Brownian motion attributed to the higher kinetic energy increasing the change of collision between particles (Mui et al., 2016; Weston et al., 2017; Zawrah et al., 2016). Moreover, the presence of alumina nanoparticle also resulted in the significant improvement on the thermal stability as reflected from the smaller disparity between data obtained across the temperature range.
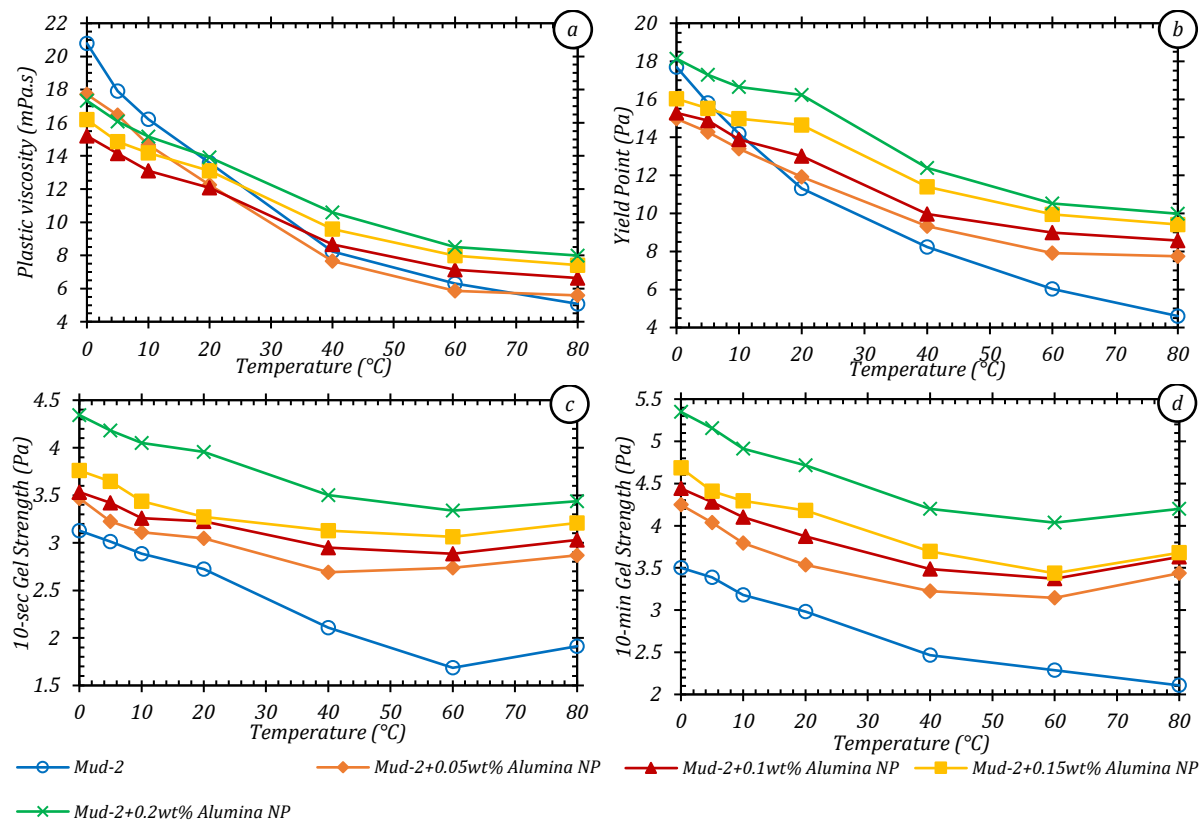

Figure 11 Results of the (a) plastic viscosity, (b) yield point, and (c) the 10-second and (d) 10-minute gel strengths of the saltwater-based muds containing various concentrations of alumina nanoparticle over temperature range between 0 and 80°C

Results on the gel strengths also gave a validation on the improved thermal stability from the addition of alumina nanoparticles, as illustrated in Figure 11c and d. The addition of alumina nanoparticles provided a treatment against the negative impact of salt ions on the mud rheological properties. As indicated in the graph, the low gel strengths observed from the Mud-2 especially at high temperatures were caused by the presence of salt ions in the mud suspension reducing the hydration capacity of the clay mineral. With the addition of alumina nanoparticle as low as 0.05 wt%, significant improvements were observed on both 10-second and 10-minute gel strengths to the more acceptable range to provide good carrying ability, i.e., 5 Pa as suggested by Machado et al., 1990. An increasing trend was also observed as the concentration of alumina increases. Biggest improvements were observed from the sample containing 0.2wt% of alumina at the temperature of 0°C, increasing up to 39% and 53% on the 10-second and 10-minute gels, as shown in Figure 11c and d, respectively. Meanwhile, at 80°C, the

respective gel strengths of the same sample increased of up to 80% and 116% flattening the curve and exhibiting the more thermally stable profiles.

Results comparison of the plastic viscosity observed between the current and past studies are presented in Figure 12. Hosseini et al., 2016, conducted experiments in a polymer-based mud system with the base sample containing glycol, polyacrylamide, sodium bicarbonate, and calcium carbonate, as well as salts which consist of sodium and potassium chlorides. The alumina nanoparticles were added at a concentration of 1wt%. Mud rheological properties were evaluated under temperatures between 25 and 85°C. As indicated by the triangle-shaped data points, a reduction in plastic viscosity was indicated from the addition of alumina across the observed temperature conditions. Although, the thermal thinning behaviour of the mud did not seem to have much changed as reflected from the decreasing trend of the viscosity curve with the final reduction of 46% was observed at 85°C. As discussed earlier, this was due to the increase of the particle dispersion from the presence of alumina. It is known that the swelling capacity of the polymer-based solution is primarily governed by the interaction between salt ions and the polymeric molecules (El Karsani et al., 2014; Livney et al., 2003). However, the presence of the negatively charged alumina particles in the bulk of the solution could result in the higher repulsion between particles increasing the degree of dispersion of the mud suspension.
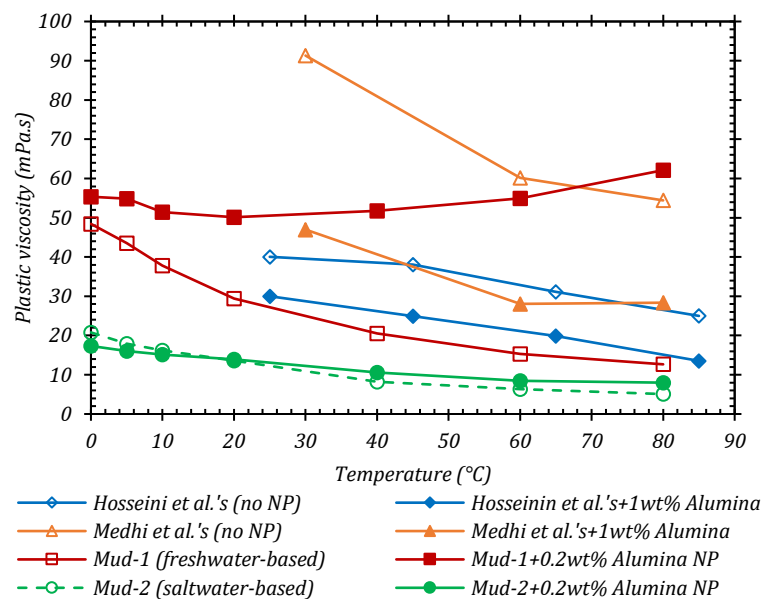

Figure 12 Results of the plastic viscosity of the water-based muds containing alumina nanoparticle from the current and past studies (Hosseini et al., 2016; Medhi et al., 2019)

As was experienced from Hosseini's results, Medhi et al., 2019, also observed a similar trend with their results. They also conducted experiments with the polymer-based drilling muds containing various types of polymers including polyacrylamide, polyamine, polyanionic cellulose, and xanthan gum. As indicated in the graph, the base sample observed a relatively high plastic viscosity of up to 91.3 mPa.s at 30°C, caused by the extensive use of polymeric solutions. The base sample also indicated a thermal thinning behaviour as the temperature increases with a plastic viscosity of 54.4 mPa.s was observed at 80°C. The addition of 1 wt% of alumina nanoparticles significantly reduced of up to 49% at 30°C with measured viscosity of 47 mPa.s. However, the presence of alumina did not seem to significantly improve mud

thermal stability as was indicated from the decreasing profile observed in plastic viscosity across the temperature conditions.

FILTRATION PROPERTIES RESULTS
Silica-Added Muds
Freshwater-based muds

Figure 13 presents the results on the filtration properties of the freshwater-based samples containing silica nanoparticles at concentrations between 0.05 and 1 wt%. In static filtration loss, spurt loss indicates the instantaneous volume of filtrate caused by the tendency of finer particles passing through the surface of a porous medium, e.g., filter paper or rock formation, before the deposition of filter cake takes place. It reflects how fast the filter cake is deposited on the surface of the filter medium. The higher the values, the slower the cake being deposited. However, it does not indicate the quality of the cake or the total volume of the filtrate (Caenn et al., 2017e). The addition of silica nanoparticles did not seem to give a significant effect on the spurt loss volume as indicated from the fairly constant trend of spurt volume as the concentration of silica increases (Figure 13a). This occurs as a result of the improved dispersion of the mud suspensions containing silica nanoparticle. It can be recalled to the discussion on the rheological section that, the addition of silica resulted in a higher particle repulsion attributed to the highly negative surface charge of particles increasing the degree of dispersion. This behaviour was also reflected in the constant trend of the spurt volume.
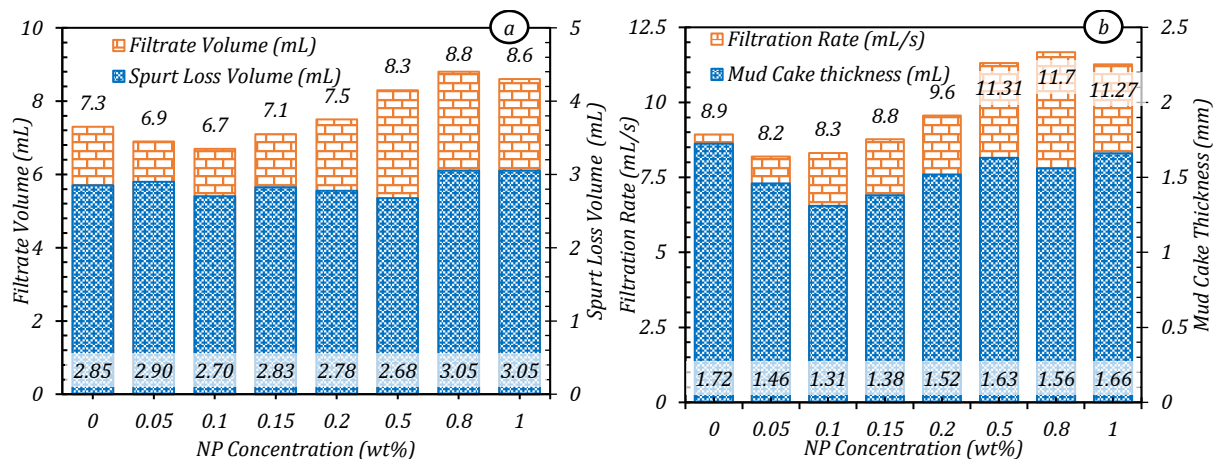

Figure 13 Filtration properties of the freshwater-based muds containing various concentrations of silica nanoparticles

However, distinct behaviour was observed on the API filtration loss, which is indicating the cumulative filtration volume measured under the 700 kPa differential pressure at ambient temperature for 30 minutes. As shown in Figure 13a, filtrate volume decreased with the increasing concentration of silica up to the concentration of 0.1 wt%, of which the filtration loss observed the biggest reduction of up to 8.2%. However, an increasing trend was then observed as the higher amount of silica present in the mud suspensions. The finding supports the proposition that have been discussed in the rheological section regarding the increasing degree of flocculation as the higher amount of silica present in the mud suspension. The increase in the filtration loss is commonly known as an indication when flocculation takes place attributed to the growing attractive force between particles (Caenn et al., 2017e).

Results on the filter cake thickness and filtration rate are presented in Figure 13b. As was experienced from the filtration volume results, reductions in the filter cake thickness were observed from the low concentrations of silica nanoparticle up to the concentration of 0.1 wt%, beyond which mud samples started to produce thicker filter cakes. As shown, the sample containing 0.1wt% produced the thinnest filter cake that corresponds to a 24% reduction from the base sample. The results on the filter cake thickness indicated a proportional trend with the filtration loss volume presented earlier. Bo et al., 1965 suggested that the thickness of filter cakes is more affected by the size and distribution of solid particles within the mud suspension, as both factors directly control the porosity, and eventually the permeability of the cake. They concluded from their results that the lower porosities were achieved from the muds containing a higher variation of particle sizes (Bo et al., 1965). The types of solid particles present in the mud suspension also contributed to the extent of cake permeability. Aggregates of particles often coexist with the higher degree of flocculation attributed to the increase of interparticle attractive forces, resulting in a stronger structure of solid particles that is more difficult to be compacted disrupting the pore bridging process (Caenn et al., 2017e). As explained earlier, particle interactions within the mud suspensions containing silica were more governed by the more dominant repulsive force rather than attraction. This, therefore, resulted in the more deflocculated suspension, thus reflected from the reduction in the filter cake thickness. As the thinner and more compacted filter cakes are built, the lower filtration rates can then be achieved. As shown in Figure 13b, the reduction in the filtration rate, especially observed from samples containing low concentrations of silica (<0.2 wt%) was also a result from the lower degree of flocculation of the silica mud suspensions. Muds containing 0.05 and 0.1 wt% of silica demonstrated the lowest filtration rate correspond to the reductions of up to 8.2% and 6.9%, respectively, from the base sample. A low rate of filtration is obtained from the bridging process that is adequately plugged the pores of the filter medium. It is also an indication of low permeability filter cakes deposited on the surface of the filter medium (Caenn et al., 2017e).

The findings regarding the role of silica nanoparticles that acts as a deflocculating agent when added into the freshwater-based drilling muds were also observed from past studies. Medhi et al., 2020, observed significant reductions in the filtration volume from the addition of 0.5 and 0.8 wt% of silica nanoparticle with a diameter range of 22 – 48 nm. As presented in Figure 14, the samples indicated reductions of up to 24% and 33%, respectively, before showing an increase of 8.7% from the sample containing 1 wt% of silica. This observation occurred when they added silica into muds containing bentonite, barite, and polyanionic cellulose. Their results confirm the highly deflocculated mud suspension with the presence of a small amount of silica (<1 wt%) (Medhi et al., 2020).
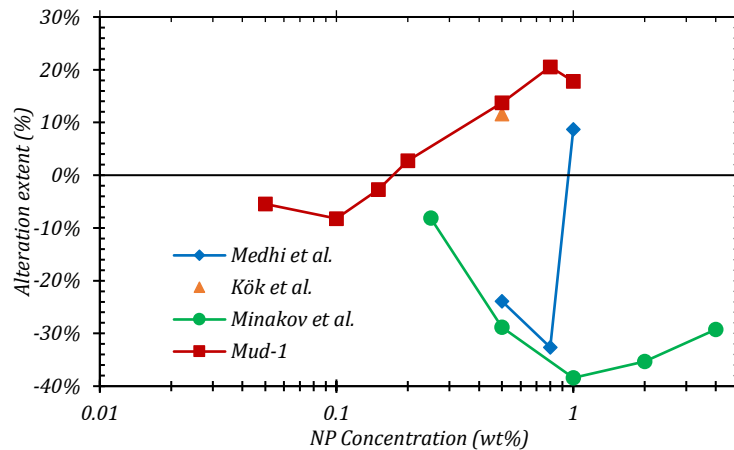
Figure 14 Alterations on the filtrate loss volume of the freshwater-based muds containing various concentrations of silica nanoparticle from the current and past studies (Kök and Bal, 2019; Medhi et al., 2020; Minakov et al., 2019)

Meanwhile, Minakov et al., 2019 also observed this typical trend from the addition of silica nanoparticle into a bentonite mud. The base sample was prepared by mixing bentonite in distilled water and aluminium nitride as a bridging agent. Silica nanoparticles were added at concentrations between 0.25 and 4 wt%, with a particle diameter of 5 nm. As also indicated in Figure 14, their results demonstrated significant reductions of up to 38% observed from the sample containing 1 wt% of silica, before indicating an increasing trend as the amount of silica increased. Another similar finding was experienced by Kök et al., 2019 when they conducted an experiment adding 0.5 wt% of silica with an average diameter of 15 – 20 nm. The base sample was prepared from mixing of distilled water, bentonite, carboxymethyl cellulose, and chrome-free lignosulfonate. The result indicated an increase of 12% in the filtrate volume, an alteration extent that was almost to what was observed from the current study.

Saltwater-based muds

Figure 15 presents the results on the filtration properties of the saltwater-based muds containing silica nanoparticles. As it was observed from the freshwater-based muds, the results on the spurt volume showed a fairly constant value up to a silica concentration of 0.2 wt%, beyond which a gradual increase started to show as the more amount of silica present in the muds (Figure 15a). This is caused by the growing trend of flocculation and aggregation at higher concentrations of nanoparticles attributed to the increase of interparticle attractive forces. Consequently, particles are more difficult to bridge the filter pores leaving an adequate and compacted filter cake more slowly to be deposited, hence resulting in higher spurt losses. Meanwhile, the cumulative filtrate loss volume indicated slight reductions of up to 11% observed from the sample containing 0.1wt% of silica, above which concentration, filtrate volume indicated an increasing trend with final 92% increase was observed at silica concentration of 1 wt%. The similar trend continued to be observed on the filter cake thickness and filtration rate, as shown in Figure 15b. The most significant reduction in the filter cake was observed from the sample of 0.1 wt% silica with a thickness of 0.98 mm corresponding to a 12.5% reduction. Meanwhile, the sample containing 0.05 wt% of silica observed the lowest filtration rate of 11.8 mL/s corresponding to an 11.2% reduction.
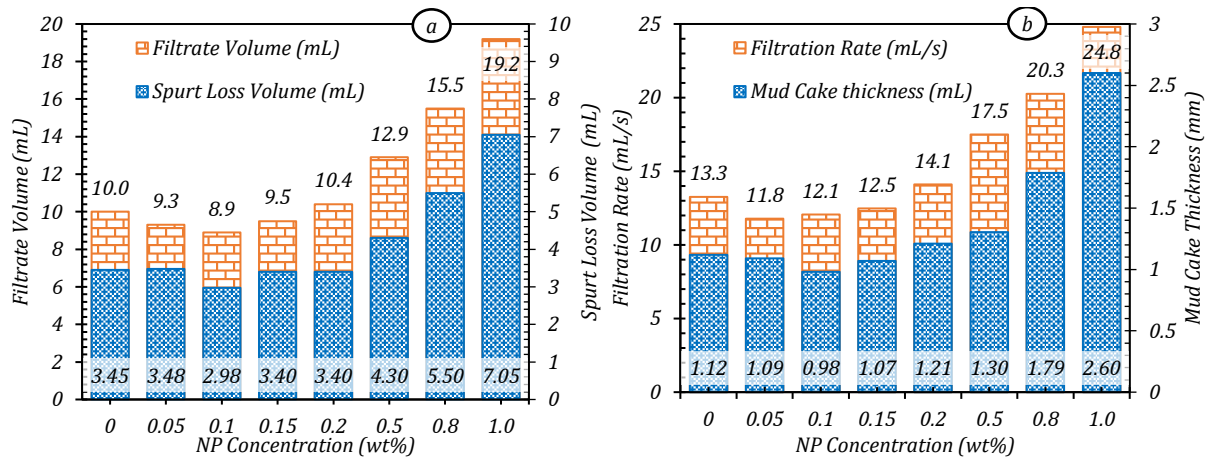
Figure 15 Filtration properties of the saltwater-based muds containing various concentrations of silica nanoparticles

As discussed earlier, the presence of salt ions promotes an even higher degree of flocculation than that of the freshwater-based system, by shrinking the double layer of particles that causes higher attractive forces. Salt ions also reduces the swelling capacity of the clay minerals by disrupting the hydrogen bonding of water molecules on the clay basal surface layers, increasing the tendency of clay platelets to aggregate, hence, resulting in poor filtration properties. However, the low filtration properties observed from samples containing lower concentrations of silica might be due to the smaller size of the created aggregates. The higher the concentration of nanoparticle, the bigger the aggregates that would be formed (Wang et al., 2012). Bigger aggregates normally have a stronger structure that makes them more difficult to be compacted creating more loose filter cake deposit with high permeability. Hence, resulting in poorer filtration properties. As shown in Figure 15b, the sample containing 1wt% of silica produced a filter cake up to 2.6 mm thick, more than 132% increase from the base sample, whilst the filtration rate demonstrated an 87% increase at 24.8 mL/s. These high extents of filtration properties indicted a poor bridging of particles producing less compacted and more permeable filter cake, resulting in an excessive volume of filtrate passing through the filter medium.

One of the past studies investigating the filtration properties of the salt-based muds was conducted by Medhi et al., 2020. In their experiments, they also added silica nanoparticles to the polymer-salt-based muds as well as in the freshwater-based system as discussed in the earlier section of this chapter. The polymer-salt-based muds were prepared without using clay materials, instead, they used a mixed variety of polymers which consisted of partially hydrolysed polyacrylamide, polyanionic cellulose, xanthan gum, and polyamine. The base sample also contained soda ash, sodium chloride, and biocide. Silica was added at concentrations of 0.5, 0.8, and 1 wt%. As presented in Figure 16, filtrate volumes were reduced with the presence of silica nanoparticles, with the final sample containing 1wt% of silica indicated a reduction of up to 69%. The reduction was observed due to the increase in the degree of dispersion of the mud suspension from the presence of the highly negatively charged silica particles.
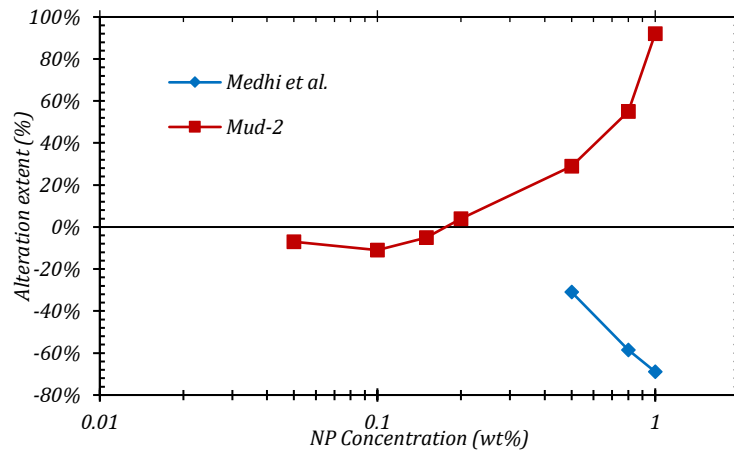
Figure 16 Alterations on the filtrate loss volume of the saltwater-based muds containing various concentrations of silica nanoparticle from Medhi et al., 2020 and the current study

In the bentonite-based muds, polymers are normally added to increase rheological properties of muds attributed to their ability to bridge and crosslink clay minerals with other solid particles within the mud suspension. However, in the absence of clay materials, mud rheology completely depends on the gelation capacity of the high molecular chains of the polymers, which might be disrupted by the addition of particle with a high negative surface charge like silica (El Karsani et al., 2014; Jia et al., 2016). Consequently, stronger interparticle repulsion was obtained increasing the degree of dispersion, which resulted in the reduction in the filtration properties of the muds.

Alumina-Added Muds

Freshwater-based muds

Results on the filtration properties of the freshwater-based muds containing alumina nanoparticles are presented in Figure 17. As shown Figure 17a, significant rises in spurt loss were observed as the concentration of alumina increases, with big increases of 107% and 212% were obtained from the samples containing 0.05 and 0.2 wt%, respectively. A similar behaviour was also indicated from the results on the total filtration loss volume, which showed rapid increases with the increasing concentration of alumina. Increases of 30% and 114% were observed from the samples containing 0.05 and 0.2 wt% of alumina nanoparticles. Again, the high degree of flocculation was behind this considerable increase in the filtrate volume. As it was discussed in the rheological section, the attractive force is more dominant in the dispersion of alumina attributed to the lower electrostatic charge of particle than the silica dispersion, increasing the tendency of particles to creates aggregates which prevent them from properly bridge the pores and quickly build an adequate filter cake. This was also confirmed from the results on the filter cake thickness presented in Figure 17b. As shown, thicker filter cakes were obtained with the addition of alumina into the mud formulation. Filter cake with 3.15 mm thickness was observed at sample containing 0.2 wt% of alumina corresponding to an 82.5% increase from the base sample. moreover, the sample also showed a high rate of filtration up to 13.7 ml/s or a 53.4% increase than that of the base sample.
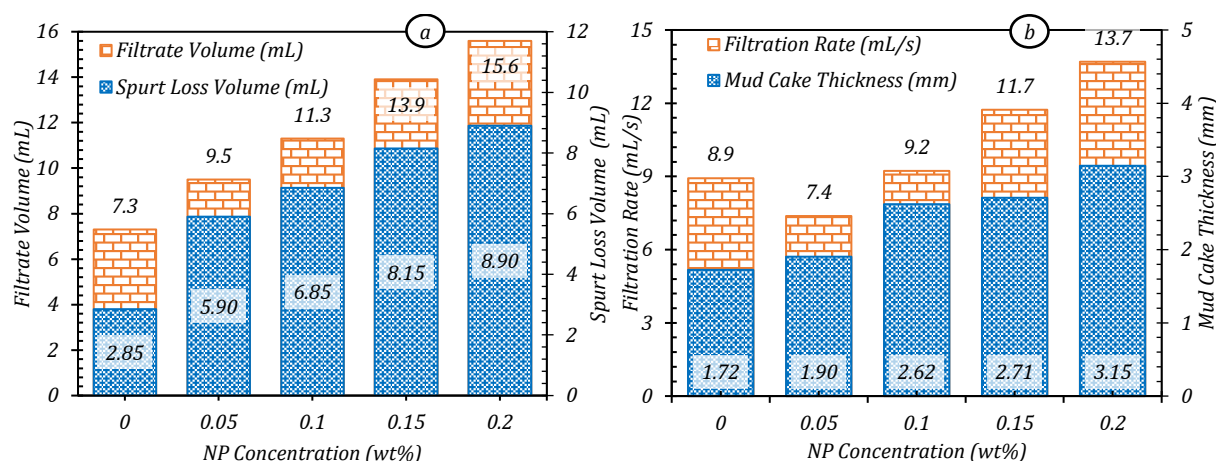
Figure 17 Filtration properties of the freshwater-based muds containing various concentrations of alumina nanoparticles

Saltwater-based muds

Results on the filtration properties of the saltwater-based muds containing alumina nanoparticles are presented in Figure 18. The spurt and total filtrate volumes demonstrated significant increases of 46% and 17%, respectively, from the addition of 0.05wt% of alumina nanoparticle. A more moderate increase was then observed on both properties as the concentration of alumina increases, with final rises of 74% and 39% in the spurt and total filtrate, respectively, were obtained from the sample containing 0.2 wt% of alumina nanoparticles, as shown in Figure 18a. Moreover, results on the filter cake thickness also indicated a relatively small effect over the concentration of alumina nanoparticle, as shown in Figure 18b, with the thickness of cakes between 1.39 and 1.64 mm were observed from samples at alumina concentrations between 0.05 and 0.2 wt%. So was with the results on the rate of filtration, as the samples observed fairly similar magnitudes across the entire concentrations of alumina nanoparticles.
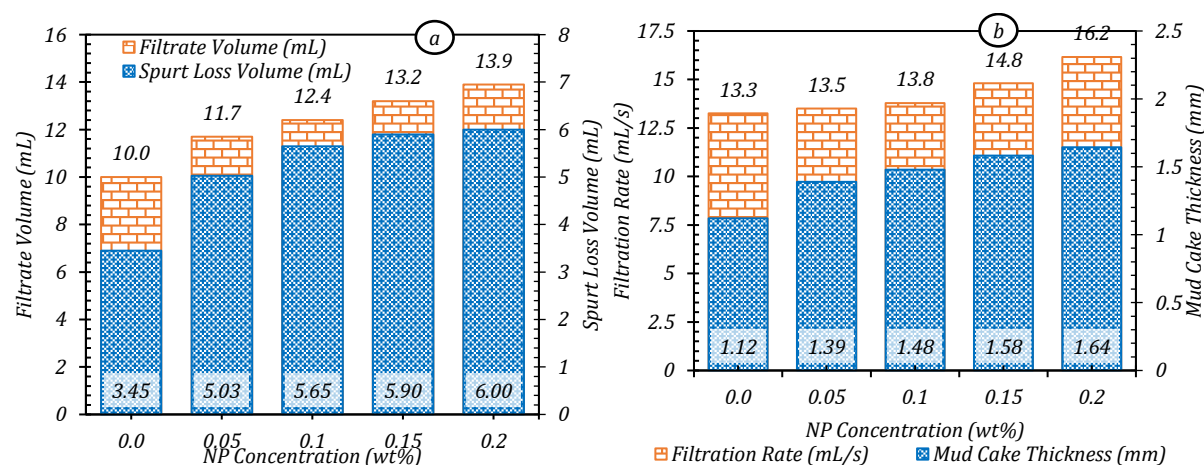

Figure 18 Results of the spurt loss and API filtrate volumes the saltwater-based muds containing various concentrations of alumina nanoparticle

The little effect on the filtration properties from the presence of alumina in saltwater-based system can be explained based on the association states of clay platelets illustrated in Figure 19. Clay materials such as bentonite, have their platelets stacked in face-to-face association in their dry state or when in reaction with moisture or water without any agitation or shearing applied to them, creating a structure that looks like a deck of cards, this state is termed as

aggregation. When high shear rates are applied, the hydrated and swollen packets will be broken apart into their individual platelets, disorientated and evenly distributed within the suspension, which then termed as dispersion. This state will be retained or improved as long as the shearing force continues. Meanwhile, when the shearing force is stopped, the suspension of clay platelets will be slowly attracted to each other creating an edge-to-edge or edge-to-face associations or combination of both resulting in a structure similar to a house of cards. This term is called flocculation. A chemical thinner (deflocculating agent) is sometimes added to neutralise the positive edge charges on clay platelets and the suspension is now in the deflocculated state. When strong electrolytes are present in the clay suspension, the cations will be adsorbed on to the clay surface and shrinking the hydration bond with water molecules promoting a higher degree of flocculation or even creates stronger aggregates when water is completely displaced from the interlayer surfaces of clay platelets (Caenn et al., 2017c; Garrison, 1939; Garrison and Ten Brink, 1940).

In the freshwater system, the base sample was in a less flocculated state resulted in the lower and more controllable filtrations as observed from the results presented Figure 17. As the concentration of alumina increases, alumina particles were drawn on to the edge surface of the clay platelets (Mui et al., 2016), forming the *house of card* structure and increasing the flocculation rate of the mud suspension. Thus, the rapid increase in the filtrations was then observed with the increasing amount of alumina nanoparticles existed in the mud suspension. On the other hand, in the saltwater-based system, the base sample was already in a higher flocculated state due to the presence of salt ions compressing the hydration layer of the clay mineral. Aggregates might also have formed indicated from the higher extents of the overall filtration properties of the base sample shown in Figure 18. The addition of alumina particles causes an increase in the filtration properties, but at smaller extents than those of the freshwater-based muds. For instance, only 39% increase in the filtrate volume was observed from saltwater mud with 0.2 wt% of alumina, compared to 114% increase observed from freshwater mud containing the same concentration of alumina. This was simply due to the reduced number of clay surfaces available for particle interaction. Besides, the amount of the readily available cations was also reduced due to the high adsorption capacity of clay basal surfaces, resulting in a less significant increase of flocculation from the presence of alumina particles.
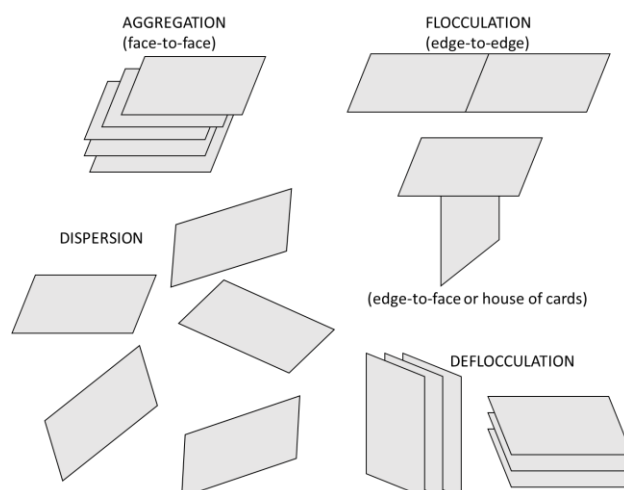
Figure 19 Oversimplified illustration on the types of platelets associations (redrawn from Bourgoyne, 1991)

SUMMARIES OF RESULTS

The results of the rheological and filtration properties evaluations of the aqueous-based drilling muds containing silica and alumina nanoparticles are summarised in the following tables.

Table 8 Summary of the rheological properties results

Mud System	Silica Nanoparticles	Alumina Nanoparticles
Freshwater-based mud	- *PV decreases steadily with increasing concentration* - *YP decreases gradually up to concentration of 0.8 wt%, then slightly increases* - *GSs drop rapidly at concentration of 0.05 wt% then increases steadily with increasing concentration*	- *PV and YP increase significantly with increasing concentration* - *GSs increase slightly with increasing concentration*
Saltwater-based mud	- *PV decreases slightly up to concentration of 0.2 wt% then increases slowly as concentration increases* - *YP and GSs increase gradually with increasing concentration*	- *PV decreases slightly up to concentration of 0.1 wt% then increased steadily with increasing concentration* - *YP and GSs increase steadily with increasing concentration*

Table 9 Summary of the filtration properties results

Mud System	Silica Nanoparticles	Alumina Nanoparticles
Freshwater-based mud	- *Spurt loss volume remains relatively stable with increasing concentration* - *Filtrate volume and mud cake thickness decrease slightly up to concentration of 0.1 wt% then increase gradually with increasing concentration* - *Rate of filtration decreases slightly at concentration of 0.05 wt% then increased steadily with increasing concentration*	- *Spurt loss volume and total filtrate volume increase significantly with increasing concentration* - *Mud cake thickness and rate of filtration increase gradually with increasing concentration*
Saltwater-based mud	- *Spurt loss volume remains relatively stable up to concentration of 0.2 wt% then increases with increasing concentration* - *Filtrate volume and mud cake thickness decrease slightly up to concentration of 0.1 wt% then increase significantly with increasing concentration* - *Rate of filtration decreases slightly at concentration of 0.05 wt% then increased significantly with increasing concentration*	*Overall filtration properties increase gradually with increasing concentration*

CONCLUSIONS AND RECOMMENDATIONS

This research aimed to investigate and design a more environmentally friendly drilling mud in the aqueous-based system with the addition of silica and alumina nanoparticles to generate a more thermally stable behaviour both at low and high temperature conditions. Silica and alumina nanoparticles at various mass concentrations were added in the preparation of the freshwater and saltwater-based drilling muds. After analysing the rheological and filtration properties results, several conclusions can be drawn as follows.

- The addition of silica and alumina nanoparticles showed an enhancement on the thermal stability indicated from the more constant rheological properties across the temperatures of 0 - 80°C as compared to those of the Base sample. Nanoparticle concentration of 0.1 wt% of both silica and alumina exhibited the most optimised characteristics in both freshwater and saltwater-based systems.
- The silica nanoparticle concentration of 0.1 wt% also exhibited the lowest filtration properties both in the freshwater and saltwater-based mud systems indicating reductions of 8.2% and 11% in the filtration loss volume, respectively, attributed to the better dispersion of particles in the mud suspension, hence lowering the degree of flocculation. On the other hand, mud samples containing alumina nanoparticles indicated an increasing trend on the filtration properties with the increasing nanoparticle concentration caused by the higher degree of flocculation attributed to the stronger interparticle attractive force.

This research has covered some part of the extensive investigations required for any alternative additives in drilling muds. Therefore, some recommendations for further research include:

- Rheological and filtration properties investigations using apparatus that can accommodate more complex conditions, e.g., low temperature and high pressure, high temperature and high pressure, for more complex compositions of drilling muds
- Investigations on the fluid dynamics and convective heat transfers of drilling muds especially to understand how the heat released from mud circulation affects surrounding Arctic environments

ACKNOWLEDGEMENT

NOMENCLATURES

μ_B	Bingham plastic viscosity or PV (mPa.s)
τ_y	Bingham yield point or YP (Pa)
ΔP	Pressure drop (kPa)
ρ	Density (kg/m^3)
Abbreviations	
ECD	Equivalent circulating density (ppg)
GS	Gel strength (Pa)
PV	Bingham plastic viscosity (mPa.s)
YP	Bingham yield point (Pa)
API	American Petroleum Institute
HPHT	High pressure -high temperature
NP	Nanoparticles
ppg	lbm/gal
ppb	lbm/bbl
psi	Pounds per square inch

REFERENCES

Abdo, J., 2014. Nano-attapulgite for improved tribological properties of drilling fluids. Surf. Interface Anal. 46, 882–887. doi:10.1002/sia.5472

Abdo, J., Al-Sharji, H., Hassan, E., 2016. Effects of nano-sepiolite on rheological properties and filtration loss of water-based drilling fluids. Surf. Interface Anal. doi:10.1002/sia.5997

Abdo, J., Haneef, M.D., 2013. Clay nanoparticles modified drilling fluids for drilling of deep hydrocarbon wells. Appl. Clay Sci. 86, 76–82. doi:10.1016/j.clay.2013.10.017

Abdo, J., Haneef, M.D., 2012. Nano-enhanced drilling fluids: Pioneering approach to overcome uncompromising drilling problems. J. Energy Resour. Technol. Trans. ASME 134. doi:10.1115/1.4005244

Abdo, J., Zaier, R., Hassan, E., Al-Sharji, H., Al-Shabibi, A., 2014. ZnO-clay nanocomposites for enhance drilling at HTHP conditions. Surf. Interface Anal. 46, 970–974. doi:10.1002/sia.5454

Adair, J.H., Suvaci, E., Sindel, J., 2001. Surface and Colloid Chemistry, in: Buschow, K.H.J., Cahn, R.W., Flemings, M.C., Ilschner, B., Kramer, E.J., Mahajan, S., Veyssière, P. (Eds.), Encyclopedia of Materials: Science and Technology. Elsevier, Oxford, pp. 1–10. doi:https://doi.org/10.1016/B0-08-043152-6/01622-3

Ahmed A, Sharifi Haddad A, Rafati R, Bashir A, AlSabagh AM, Aboulrous AA. Developing a Thermally Stable Ester-Based Drilling Fluid for Offshore Drilling Operations by Using Aluminum Oxide Nanorods. Sustainability. 2021; 13(6):3399.

Barry, M.M., Jung, Y., Lee, J.-K., Phuoc, T.X., Chyu, M.K., 2015. Fluid filtration and rheological properties of nanoparticle additive and intercalated clay hybrid bentonite

drilling fluids. J. Pet. Sci. Eng. 127, 338–346. doi:http://dx.doi.org/10.1016/j.petrol.2015.01.012

Bashir, A, Haddad, A.S, Rafati, R, Nanoparticle/polymer-enhanced alpha olefin sulfonate solution for foam generation in the presence of oil phase at high temperature conditions, Colloids and Surfaces A: Physicochemical and Engineering Aspects, Volume 582, 2019, 123875.

Bayat[a], A.E., Junin, R, Samsuri A, Piroozian A, Hokmabadi, M, Impact of Metal Oxide Nanoparticles on Enhanced Oil Recovery from Limestone Media at Several Temperatures, Energy Fuels 2014, 28, 10, 6255–6266.

Bayat[b], A.E., Shams, R., 2019. Appraising the impacts of SiO2, ZnO and TiO2 nanoparticles on rheological properties and shale inhibition of water-based drilling Muds. Colloids and Surfaces A: Physicochemical and Engineering Aspects 581, 123792 doi:10.1016/j.colsurfa.2019.123792#

Bayat[c], A.E, Moghanloo, P.J, Piroozian, A, Rafati, R, Experimental investigation of rheological and filtration properties of water-based drilling fluids in presence of various nanoparticles, Colloids and Surfaces A: Physicochemical and Engineering Aspects, Volume 555, 2018, Pages 256-263.

Ben-Nissan, B., Choi, A.H., Cordingley, R., 2008. Alumina ceramics, in: Bioceramics and Their Clinical Applications. Elsevier Inc., pp. 223–242. doi:10.1533/9781845694227.2.223

Bo, M., Freshwater, D., Scarlett, B., 1965. Effect of Particle-Size Distribution on Permeability of Filter Cakes. Trans. Inst. Chem. Eng.

Bourgoyne, A.T., 1991. Applied drilling engineering. Society of Petroleum Engineers, Richardson, TX.

Caenn, R., Darley, H.C.H., Gray, G.R., 2017a. Chapter 5 - Water-Dispersible Polymers, in: Caenn, R., Darley, H.C.H., Gray, G.R. (Eds.), Composition and Properties of Drilling and Completion Fluids (Seventh Edition). Gulf Professional Publishing, Boston, pp. 135–150. doi:https://doi.org/10.1016/B978-0-12-804751-4.00005-5

Caenn, R., Darley, H.C.H., Gray, G.R., 2017b. Chapter 6 - The Rheology of Drilling Fluids, in: Caenn, R., Darley, H.C.H., Gray, G.R. (Eds.), Composition and Properties of Drilling and Completion Fluids (Seventh Edition). Gulf Professional Publishing, Boston, pp. 151–244. doi:https://doi.org/10.1016/B978-0-12-804751-4.00006-7

Caenn, R., Darley, H.C.H., Gray, G.R., 2017c. Chapter 4 - Clay Mineralogy and the Colloid Chemistry of Drilling Fluids, in: Composition and Properties of Drilling and Completion Fluids. Gulf Professional Publishing, Boston, pp. 93–134.

Caenn, R., Darley, H.C.H., Gray, G.R., 2017d. Chapter 10 - Drilling Problems Related to Drilling Fluids, in: Caenn, R., Darley, H.C.H., Gray, G.R. (Eds.), Composition and Properties of Drilling and Completion Fluids (Seventh Edition). Gulf Professional Publishing, Boston, pp. 367–460. doi:https://doi.org/10.1016/B978-0-12-804751-4.00010-9

Caenn, R., Darley, H.C.H., Gray, G.R., 2017e. Chapter 7 - The Filtration Properties of Drilling Fluids, in: Caenn, R., Darley, H.C.H., Gray, G.R. (Eds.), Composition and Properties of Drilling and Completion Fluids (Seventh Edition). Gulf Professional Publishing, Boston, pp. 245–283. doi:https://doi.org/10.1016/B978-0-12-804751-4.00007-9

Çınar, S., Akinc, M., 2014. Electrostatic Stabilization of Alumina Nanopowder Suspensions. Sci. Adv. Mater. 6, 520–529. doi:10.1166/sam.2014.1773

Davison, J.M., Clary, S., Saasen, A., Allouche, M., Bodin, D., Nguyen, V.-A., 1999. Rheology of Various Drilling Fluid Systems Under Deepwater Drilling Conditions and the Importance of Accurate Predictions of Downhole Fluid Hydraulics. doi:10.2118/56632-MS

Dejtaradon, P, Hamidi, H, Chuks, M.H, Wilkinson, D, Rafati, R, Impact of ZnO and CuO nanoparticles on the rheological and filtration properties of water-based drilling fluid, Colloids and Surfaces A: Physicochemical and Engineering Aspects, Volume 570, 2019, Pages 354-367.

Dickson, A.G., Goyet, C., 1994. Handbook of Methods for the Analysis of the Various Parameters of the Carbon Dioxide System in Sea Water.

El Karsani, K.S.M., Al-Muntasheri, G.A., Sultan, A.S., Hussein, I.A., 2014. Impact of salts on polyacrylamide hydrolysis and gelation: New insights. J. Appl. Polym. Sci. 131. doi:10.1002/app.41185

Elward-Berry, J., Thomas, E.W., 1994. Rheologically Stable Deepwater Drilling Fluid Development and Application. doi:10.2118/27453-MS

Friedheim, J., Lee, J., Young, S., Cullum, D., 2011. New Thermally Independent Rheology Invert Drilling Fluid For Multiple Applications.

Garrison, A.D., 1939. Surface Chemistry of Clays and Shales. Trans. AIME 132, 191–204. doi:10.2118/939191-G

Garrison, A.D., Ten Brink, K.C., 1940. A Study of Some Phases of Chemical Control in Clay Suspensions. Trans. AIME 136, 175–194. doi:10.2118/940175-g

Hassani, S.S., Amrollahi, A., Rashidi, A., Soleymani, M., Rayatdoost, S., 2016. The effect of nanoparticles on the heat transfer properties of drilling fluids. J. Pet. Sci. Eng. 146, 183–190. doi:http://dx.doi.org/10.1016/j.petrol.2016.04.009

Hendraningrat, L., Li, S., Torsæter, O., 2013. A coreflood investigation of nanofluid enhanced oil recovery. J. Pet. Sci. Eng. 111, 128–138. doi:http://dx.doi.org/10.1016/j.petrol.2013.07.003

Hilfiger, M.G., Thaemlitz, C.J., Moellendick, E., 2016. Investigating the Chemical Nature of Flat Rheology. doi:10.2118/180320-MS

Hosseini, S., Farahbod, F., Zargar, G., 2016. The Study of Effective of Added Aluminum Oxide Nano Particles to the Drilling Fluid: The Evaluation of Two Synthesis Methods. J Pet Env. Biotechnol 7, 3. doi:10.4172/2157-7463.1000283

Ivanov, D.A., Sitnikov, A.I., Semenychev, S.S., Fomina, G.A., 1999. Heat resistance of alumina ceramics. Refract. Ind. Ceram. 40, 14–18. doi:10.1007/BF02762437

Jailani, S., Franks, G.V., Healy, T.W., 2008. ζ Potential of Nanoparticle Suspensions: Effect of Electrolyte Concentration, Particle Size, and Volume Fraction. J. Am. Ceram. Soc. 91, 1141–1147. doi:10.1111/j.1551-2916.2008.02277.x

Jain, R., Mahto, V., Sharma, V.P., 2015. Evaluation of polyacrylamide-grafted-polyethylene glycol/silica nanocomposite as potential additive in water based drilling mud for reactive shale formation. J. Nat. Gas Sci. Eng. 26, 526–537. doi:10.1016/j.jngse.2015.06.051

Jia, H., Ren, Q., Li, Y.M., Ma, P., 2016. Evaluation of polyacrylamide gels with accelerator ammonium salts for water shutoff in ultralow temperature reservoirs: Gelation performance and application recommendations. Petroleum 2, 90–97. doi:10.1016/j.petlm.2015.12.003

Katiyar, P., Singh, J.K., 2018. The effect of ionisation of silica nanoparticles on their binding to nonionic surfactants in oil–water system: an atomistic molecular dynamic study. Mol. Phys. 116, 2022–2031. doi:10.1080/00268976.2018.1456683

Knox, D., Bulgachev, R., Cameron, I., 2015. Defining fragile - The challenge of engineering drilling fluids for narrow ECD windows, in: SPE/IADC Drilling Conference. Society of Petroleum Engineers, pp. 838–854.

Kök, M.V., Bal, B., 2019. Effects of silica nanoparticles on the performance of water-based drilling fluids. J. Pet. Sci. Eng. 180, 605–614. doi:https://doi.org/10.1016/j.petrol.2019.05.069

Kumar, A., Dixit, C.K., 2017. Methods for characterization of nanoparticles, in: Advances in

Nanomedicine for the Delivery of Therapeutic Nucleic Acids. Elsevier Inc., pp. 44–58. doi:10.1016/B978-0-08-100557-6.00003-1

Larsson, R., Andersson, O., 2000. Lubricant thermal conductivity and heat capacity under high pressure. Proc. Inst. Mech. Eng. Part J J. Eng. Tribol. 214, 337–342. doi:10.1243/1350650001543223

Lee, J., Cullum, D., Friedheim, J., Young, S., 2012. A new SBM for narrow margin extended reach drilling, in: SPE/IADC Drilling Conference. Society of Petroleum Engineers, pp. 1106–1116.

Livney, Y.D., Portnaya, I., Faupin, B., Ramon, O., Cohen, Y., Cogan, U., Mizrahi, S., 2003. Interactions between inorganic salts and polyacrylamide in aqueous solutions and gels. J. Polym. Sci. Part B Polym. Phys. 41, 508–519. doi:10.1002/polb.10406

Machado, J.C.V., Aragao, A.F.L., 1990. Gel Strength as Related to Carrying Capacity of Drilling Fluids, in: SPE Latin America Petroleum Engineering Conference. Society of Petroleum Engineers. doi:10.2118/21106-MS

Mahian, O., Kolsi, L., Amani, M., Estellé, P., Ahmadi, G., Kleinstreuer, C., Marshall, J.S., Siavashi, M., Taylor, R.A., Niazmand, H., Wongwises, S., Hayat, T., Kolanjiyil, A., Kasaeian, A., Pop, I., 2019. Recent advances in modeling and simulation of nanofluid flows-Part I: Fundamentals and theory. Phys. Rep. doi:10.1016/j.physrep.2018.11.004

Mahmoud, O., Nasr-El-Din, H.A., Vryzas, Z., Kelessidis, V.C., 2016. Nanoparticle-Based Drilling Fluids for Minimizing Formation Damage in HP/HT Applications. SPE Int. Conf. Exhib. Form. Damage Control. doi:10.2118/178949-MS

Mao, H., Qiu, Z., Shen, Z., Huang, W., 2015. Hydrophobic associated polymer based silica nanoparticles composite with core–shell structure as a filtrate reducer for drilling fluid at utra-high temperature. J. Pet. Sci. Eng. 129, 1–14. doi:http://dx.doi.org/10.1016/j.petrol.2015.03.003

Maunder, T.E., Le, K.M., Miller, D.L., 1990. Drilling Waste Disposal in the Arctic Using Below-Grade Freezeback. doi:10.2118/20429-MS

Medhi, S., Chowdhury, S., Dharmender Kumar, G., Mazumdar, A., 2020. An investigation on the effects of silica and copper oxide nanoparticles on rheological and fluid loss property of drilling fluids. J. Pet. Explor. Prod. Technol. 10, 91–101. doi:http://dx.doi.org/10.1007/s13202-019-0721-y

Medhi, S., Chowdhury, S., Sangwai, J.S., Gupta, D.K., 2019. Effect of Al2O3 nanoparticle on viscoelastic and filtration properties of a salt-polymer-based drilling fluid. Energy Sources, Part A Recover. Util. Environ. Eff. doi:10.1080/15567036.2019.1662140

Metin, C.O., Lake, L.W., Miranda, C.R., Nguyen, Q.P., 2011. Stability of aqueous silica nanoparticle dispersions. J. Nanoparticle Res. 13, 839–850. doi:10.1007/s11051-010-0085-1

Minakov, A. V, Mikhienkova, E.I., Voronenkova, Y.O., Neverov, A.L., Zeer, G.M., Zharkov, S.M., 2019. Systematic experimental investigation of filtration losses of drilling fluids containing silicon oxide nanoparticles. J. Nat. Gas Sci. Eng. 71, 102984. doi:https://doi.org/10.1016/j.jngse.2019.102984

Mui, J., Ngo, J., Kim, B., 2016. Aggregation and colloidal stability of commercially available Al2O3 nanoparticles in aqueous environments. Nanomaterials 6. doi:10.3390/nano6050090

Nadolny, Z., Dombek, G., 2017. Thermal properties of mixtures of mineral oil and natural ester in terms of their application in the transformer. E3S Web Conf. 19, 01040. doi:10.1051/e3sconf/20171901040

Nesbitt, L.E., Sanders, J.A., 1981. Drilling Fluid Disposal. J. Pet. Technol. doi:10.2118/10098-PA

Norrish, K., 1954. The swelling of montmorillonite. Discuss. Faraday Soc. 18, 120–134.

doi:10.1039/DF9541800120

Oh, M.-H., So, J.-H., Lee, J.-D., Yang, S.-M., 1999a. Preparation of Silica Dispersion and its Phase Stability in the Presence of Salts, Korean .1. Chem. Eng.

Oh, M.-H., So, J.-H., Yang, S.-M., 1999b. Rheological Evidence for the Silica-Mediated Gelation of Xanthan Gum. J. Colloid Interface Sci. 216, 320–328. doi:https://doi.org/10.1006/jcis.1999.6325

Omurlu, C., Pham, H., Nguyen, Q.P., 2016. Interaction of surface-modified silica nanoparticles with clay minerals. Appl. Nanosci. 6, 1167–1173. doi:10.1007/s13204-016-0534-y

Oyekunle, L.O., Susu, A.A., 2005. High Temperature Thermal Stability Investigation of Paraffinic Oil. Pet. Sci. Technol. 23, 199–207. doi:10.1081/LFT-200028179

Pabley, A.S., 1985. Saltwater and hard water bentonite mud. US 4500436.

Patel, C.M., Chakraborty, M., Murthy, Z.V.P., 2015. Influence of pH on the Stability of Alumina and Silica Nanosuspension Produced by Wet Grinding. Part. Sci. Technol. 33, 240–245. doi:10.1080/02726351.2014.978425

Rafati, R, Smith, S.R, Haddad, A.S, Novara,R, Hamidi, H, Effect of nanoparticles on the modifications of drilling fluids properties: A review of recent advances,, Journal of Petroleum Science and Engineering, Volume 161, 2018, Pages 61-76.

Rakhmangulov, R., Evdokimova, I., Dobrokhleb, P., Chettykvayeva, K., Zadvornov, D., Kretsul, V., Borodai, A., Ageeva, E., Gulov, A., Zhuravchak, V., Zhludov, A., Novikov, S., 2016. Entering the Arctic Gate: High End Drilling at the High Latitude. SPE Russ. Pet. Technol. Conf. Exhib. doi:10.2118/181922-MS

Rojas, J.C., Daugherty, W.T., Irby, R.D., Bern, P.A., Romo, L.A., Dye, W.M., Greene, B., Trotter, R.N., 2007. New Constant-Rheology Synthetic-Based Fluid Reduces Downhole Losses in Deepwater Environments. doi:10.2118/109586-MS

Sadeghalvaad, M., Sabbaghi, S., 2015. The effect of the TiO2/polyacrylamide nanocomposite on water-based drilling fluid properties. Powder Technol. 272, 113–119. doi:10.1016/j.powtec.2014.11.032

Smith, S.R, Rafati, R, Haddad, A.S, Cooper, A, Hamidi, H, Application of aluminium oxide nanoparticles to enhance rheological and filtration properties of water based muds at HPHT conditions, Colloids and Surfaces A: Physicochemical and Engineering Aspects, Volume 537, 2018, Pages 361-371.

Srivatsa, J.T., Ziaja, M.B., 2012. An experimental investigation on use of nanoparticles as fluid loss additives in a surfactant - Polymer based drilling fluid, in: International Petroleum Technology Conference. International Petroleum Technology Conference, pp. 2436–2454. doi:10.2523/IPTC-14952-MS

Taraghikhah, S., Kalhor Mohammadi, M., Tahmasbi Nowtaraki, K., 2015. Multifunctional Nanoadditive in Water Based Drilling Fluid for Improving Shale Stability. Int. Pet. Technol. Conf. 2015. doi:10.2523/IPTC-18323-MS

Timofeeva, E., Smith, D., Yu, W., France, D., Singh, D., Routbort, J., 2010. Particle size and interfacial effects on thermo-physical and heat transfer characteristics of water-based alpha-SiC nanofluids. Nanotechnology 21, 215703. doi:10.1088/0957-4484/21/21/215703

Tournassat, C., Bourg, I.C., Steefel, C.I., Bergaya, Faïza, 2015. Chapter 1 - Surface Properties of Clay Minerals, in: Tournassat, C., Steefel, C.I., Bourg, I.C., Bergaya, Faqpza (Eds.), Developments in Clay Science. Elsevier, pp. 5–31. doi:https://doi.org/10.1016/B978-0-08-100027-4.00001-2

Tournassat, C., Grangeon, S., Leroy, P., Giffaut, E., 2013. Modeling specific ph dependent sorption of divalent metals on montmorillonite surfaces. a review of pitfalls, recent achievements and current challenges. Am. J. Sci. 313, 395–451. doi:10.2475/05.2013.01

van Oort, E., Lee, J., Friedheim, J., Toups, B., 2004. New Flat-Rheology Synthetic-Based Mud

for Improved Deepwater Drilling. doi:10.2118/90987-MS

Vargas, J., Roldán, L., Lopera, S., Cardenas, J., Zabala, R., Franco Ariza, C., Cortés, F., 2019. Effect of Silica Nanoparticles on Thermal Stability in Bentonite Free Water-Based Drilling Fluids to Improve its Rheological and Filtration Properties After Aging Process. Offshore Technol. Conf. doi:10.4043/29901-MS

Wang, T., Mingjiang, N.I., Zhongyang, L., Chunhui, S., Kefa, C., 2012. Viscosity and aggregation structure of nanocolloidal dispersions 57, 3644–3651. doi:10.1007/s11434-012-5150-y

Weston, J.S., Harwell, J.H., Grady, B.P., 2017. Rheological characterization of yield stress gels formed: Via electrostatic heteroaggregation of metal oxide nanoparticles. Soft Matter 13, 6743–6755. doi:10.1039/c7sm01035d

William, J.K.M., Ponmani, S., Samuel, R., Nagarajan, R., Sangwai, J.S., 2014. Effect of CuO and ZnO nanofluids in xanthan gum on thermal, electrical and high pressure rheology of water-based drilling fluids. J. Pet. Sci. Eng. doi:10.1016/j.petrol.2014.03.005

Yakushev, V.S., Collett, T.S., 1992. Gas Hydrates In Arctic Regions: Risk To Drilling And Production. Int. Offshore Polar Eng. Conf.

Yapici, K., Osturk, O., Uludag, Y., 2018. Dependency of Nanofluid Rheology on Particle Size and Concentration of Various Metal Oxide Nanoparticles 35, 575–586. doi:10.1590/0104-6632.20180352s20160172

Young, S., Friedheim, J.E., Lee, J., Prebensen, O.I., 2012. A New Generation of Flat Rheology Invert Drilling Fluids. doi:10.2118/154682-MS

Zawrah, M.F., Khattab, R.M., Girgis, L.G., El Daidamony, H., Abdel Aziz, R.E., 2016. Stability and electrical conductivity of water-base Al2O3 nanofluids for different applications. HBRC J. 12, 227–234. doi:10.1016/j.hbrcj.2014.12.001